Chapter 10

EPR Oximetry in Biological and Model Samples

Witold K. Subczynski[1] and Harold M. Swartz[2]
[1]National Biomedical EPR Center,Department of Biophysics, Medical College of Wisconsin, Milwaukee, Wisconsin 53226; [2]Department of Radiology, Dartmouth Medical School, Hanover, New Hampshire 03755

Abstract: The well-known broadening of CW EPR spectra due to collision of the free radical with molecular oxygen in solution has been made into a tool for measuring oxygen concentration in numerous biological systems. The principles of the measurement of oxygen by this method are described, both for spin labels and for oxygen-sensitive particulate probes, such as coals, India ink, and lithium phthalocyanine. Applications are described for cell respiration, membrane permeability, and *in vivo* measurements on animal organs.

1. INTRODUCTION

The application of spin-label oximetry to biological and model systems dates back about 35 years. Backer et al. (1977) first emphasized that the resolution of the proton superhyperfine structure in the EPR spectrum of spin label I (Fig. 1) is very sensitive to the concentration of oxygen, and can be used as a parameter in measurements of oxygen consumption in mitochondria and cell suspensions. However, other scientists did not commonly use that spin label. Instead, spin label II (Fig. 1), obtained from Rozantzev's laboratory in Moscow, began being used more extensively, starting in early 1978 in the Department of Biophysics, Jagiellonian University, Krakow, Poland where it was employed to measure oxygen concentrations in tumor cell suspensions (Pajak et al., 1978). This spin label was later named CTPO (Popp and Hyde, 1981), which is the name commonly accepted and used in the literature. The changes of the superhyperfine structure in its EPR signal were parameterized as a function

of oxygen concentration. A useful parameter, called the "*K* parameter," was introduced by Sarna et al. (1980) (Fig. 2), and numerous calibration curves showing *K* as a function of oxygen concentration, temperature, spin label concentration, and microwave power have been published (e.g. Lai et al., 1982). Because of its high polarity, CTPO samples oxygen in the aqueous phase. A number of other spin labels that use superhyperfine structure for oximetry measurements also have been utilized (Morse et al., 1985; Chan et al. 1989), but CTPO (with the *K* parameter and Lai's calibration curves) has remained a widely used probe for oximetry measurements. It also should be that Povich (1975a; 1975b) seems to be the first who stated explicitly the important principle that the effects of oxygen on the EPR spectra measurements depend on both oxygen concentration and diffusion when using soluble free radicals for oximetry.

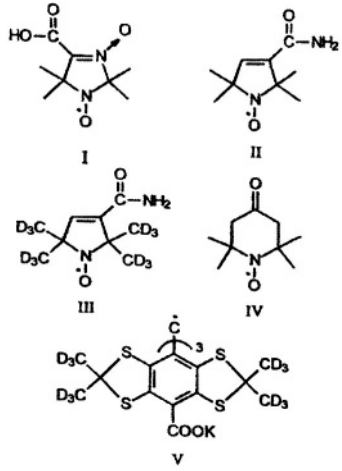

Figure 1. Chemical structures of spin-label molecular probes.

In 1980, the focus for development of EPR oximetry moved to the National Biomedical ESR Center at the Medical College of Wisconsin in Milwaukee. Here, EPR spectra of CTPO were carefully calibrated for measurement of oxygen consumption in cell suspensions during the cell cycle and during significant biochemical reactions (Sarna et al., 1980; Lai et al., 1982; Sarna and Sealy, 1984; Subczynski and Kusumi, 1985; Ankel et al., 1986; Kalyanaraman et al., 1987). It was also here that T_1 sensitive methods for evaluation of the product of oxygen diffusion-concentration in membranes were introduced and developed (Subczynski and Hyde, 1981; Kusumi et al., 1982; Yin and Hyde, 1987; Subczynski et al., 1989). It was shown that spin-label oximetry can be used as a quantitative method,

because every collision of oxygen with a spin label contributes to changes in an EPR spectrum in both T_1 and T_2 sensitive methods (Hyde and Subczynski, 1984, 1989; Subczynski and Hyde, 1981, 1984). The tremendous progress in development of spin-label oximetry was aided by the use of an oxygen permeable plastic, based on methyl pentene polymers, called TPX, for construction of sample containers, including capillaries (Popp and Hyde, 1981; Subczynski and Hyde, 1981). This facilitated equilibration of EPR samples with the desired partial pressure of oxygen. In all these developments, Professor James S. Hyde was a key individual. (Presently TPX rods can be purchased from Midland Plastic, Inc. (Madison, WI) and TPX capillaries together with the holder can be obtained from Molecular Specialties, Inc., Milwaukee, WI).

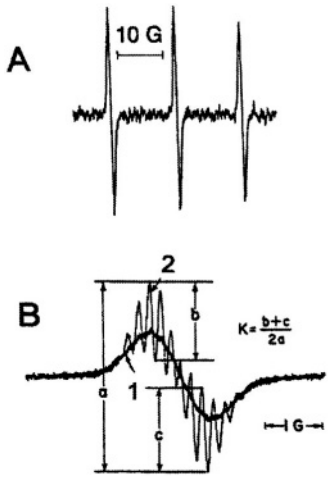

Figure 2. The EPR spectrum of an aerated solution of the 1.1×10^{-4} M CTPO in water (A). The central field component of the EPR spectrum of CTPO in air-saturated (1) and nitrogen-saturated (2) water (B). Spectra were recorded at 37°C. Definition of the *K* parameter is indicated.

The most significant contribution made by Jim Hyde, however, was in the development of T_1-sensitive oximetry methods including saturation recovery (the absolute T_1 method (Kusumi et al., 1982; Yin and Hyde, 1987; Subczynski et al., 1989)), CW saturation (Subczynski and Hyde, 1981), passage display (Froncisz et al., 1985), and the multiquantum approach (Mchaourab and Hyde, 1993; Mchaourab et al., 1994).

The contribution of Jim Hyde to *in vivo* oximetry also should be noted. His development, together with Wojciech Froncisz, of loop-gap resonators (Froncisz and Hyde, 1982) permitted measurements to be made at low

frequencies for larger water containing samples, including small laboratory animals (Lukiewicz and Lukiewicz, 1984; Lukiewicz, 1985). The first *in vivo* oximetry measurement, which is co-authored by Hyde, was done on mice (Subczynski et al., 1986). It gave significant data about changes in oxygen concentration in the peritoneal cavity when the gas the animal breathed was changed from air to pure oxygen.

Subsequently as additional *in vivo* oximetry methods based on EPR have been developed elsewhere, the National Biomedical ESR Center has continued to be involved in these developments in many important ways, including extensive interactions with the centers that are focused on this technique. In this chapter we consider both the initial method in which spin labels (nitroxides) are used as the oxygen sensitive paramagnetic probes, which is termed spin label oximetry, and the other methods that have been developed subsequently (but which have not displaced spin label oximetry). Because the *in vivo* methods of EPR oximetry have been thoroughly reviewed recently (Swartz and Clarkson, 1998; Swartz. 2003) and have not been as central to the ESR Center in Milwaukee, we have focused especially on applications to model and cellular systems in this chapter.

2. MEASUREMENT OF OXYGEN USING SPIN-LABEL PROBES

Even though molecular oxygen is paramagnetic, having a triplet ground state, no EPR spectrum has been recorded for oxygen dissolved in liquids near physiological temperatures. Fortunately, methods exist in which bimolecular collisions of molecular oxygen (paramagnetic, fast-relaxing, unobservable through EPR) with different spin-label probes (slow-relaxing, observable through EPR) are used to monitor the product of oxygen diffusion-concentration. Under appropriate conditions this product can be separated, giving the ability to measure the oxygen concentration or oxygen diffusion coefficient (Hyde et al., 1983; Hyde and Subczynski, 1989).

2.1 The Smoluchowski Equation

Because the collision between molecular oxygen and the free radical moiety of a spin label is at the heart of spin label oximetry, analyses of the EPR data are based on the Smoluchowski equation,

$$\omega = 4\,\pi r_0 (D_{SL} + D_O) C \qquad (1)$$

where r_o is the interaction distance between oxygen and nitroxide radical spin labels (4.5 Å; Windrem and Plachy, 1980) and C is the oxygen concentration expressed in molecules per unit volume. To measure the collision rate, an experimental observable, ω_{exp}, is related to the actual collision frequency, ω:

$$\omega_{exp} = 4\pi p\, r_o (D_{SL} + D_O) C \qquad (2)$$

where p is the probability that a spectroscopically observable event occurs when a collision takes place. This equation predicts how frequently a given spin-label molecule encounters surrounding oxygen molecules. It does not take into account the concentration of spin labels.

Usually the diffusion coefficient of oxygen, D_O, is much greater than the diffusion coefficient of the spin label, D_{SL}. The macroscopic diffusion coefficients of molecular oxygen in water (low viscosity environment) at 37, 20, and 10°C are 3.0×10^{-5}, 2.0×10^{-5}, and 1.5×10^{-5} $cm^2\ s^{-1}$, respectively (St. Denis and Fell, 1971). At these temperatures, values for the diffusion coefficients obtained for the smallest spin label d-Tempone in water are 0.9×10^{-5}, 0.6×10^{-5}, and 0.45×10^{-5} $cm^2\ s^{-1}$, respectively. These values were obtained from EPR line broadening data presented by Molin et al. (1980). The value of 0.72×10^{-5} $cm^2\ s^{-1}$ for translational diffusion of di-t-butyl nitroxide in water at 26°C was obtained by Ahn (1976) using a capillary diffusion method. In more viscous environment such as lipid bilayer membranes the difference between diffusion coefficient of oxygen and diffusion coefficient of lipid spin labels is much greater reaching two – three orders of magnitude (see Subczynski et al., 1984; 1986; 1992a for more data and discussion).Therefore, a useful simplification can be made by neglecting the diffusion coefficient of the spin label, relative to that of oxygen:

$$\omega_{exp} = 4\pi p\, r_o D_O C \qquad (3)$$

If this is possible, the experimental observation yields the oxygen diffusion-concentration product, $D_O C$. The interaction distance, r_o, can be adjusted to force the equality of the oxygen diffusion coefficient obtained from measuring the diffusion against a concentration gradient (macroscopic diffusion) and that from the Smoluchowski equation (self diffusion). It was shown that for spin labels, this agreement is obtained for $pr_o = 4.5$ Å (Hyde and Subczynski, 1984, 1989; Subczynski and Hyde, 1984). This is what makes the EPR spin label oximetry method quantitative.

2.2 Basic Methodological Approaches

Initially, the term *spin-label oximetry* was used to describe the application of nitroxide radical spin labels to oximetry measurements. It is now often broadened to include the use of any soluble paramagnetic substance that possesses an EPR spectrum sensitive to collisions with molecular oxygen, and occasionally even to the particulate paramagnetic probes that have been introduced, especially for *in vivo* oximetry. In this paper we reserve the use of the term to oximetry with soluble free radicals, and use the more general term "EPR oximetry" to apply to all types of oxygen-sensitive paramagnetic materials.

The three major methodological approaches used for spin-label oximetry can be classified as molecular, microscopic, and macroscopic. In the first approach, spin label molecules are directly dissolved in the examined systems. In the second and third approaches the paramagnetic material is confined. For soluble materials, the solution is confined within liposomes, proteinaceous microspheres, oil droplets, or plastic capillaries that prevent its mixing with the investigated system, while molecular oxygen can freely diffuse in and out of microscopic and macroscopic probes. Differentiating between the microscopic and macroscopic methods is somewhat arbitrary. The size of the microscopic probe should be smaller than the size of the cell (a few microns in diameter). The size of the macroscopic probe can be as large as 1 - 2 cm.

Oximetry with particulates, while having some similarities with spin label oximetry, is sufficiently different that it is useful to consider them separately. The particulates always provide localized information at the sites where the particles are located. When studies are done with a slurry of small particles, then the similarities with microscopic spin label oximetry are considerable. Most studies with particles, however, are done with macroscopic particles that are placed at one or more sites of interest. The most important role of oximetry based on the particulates is for *in vivo* oximetry in which repeated measurements from the same sites are needed.

2.2.1 Molecular Spin-Label Probes

The use of spin-label molecular probes I and II (CTPO) for oximetry has already been mentioned. Professor Howard Halpern at the 29th Rocky Mountain Conference in Denver, Colorado, described a partially deuterated CTPO analog (spin label III, Fig. 1) in August 1987. This spin label has only two resolved superhyperfine lines in its EPR spectrum, which arise from the interaction of an unpaired electron with the ring proton. This spectral feature is used to distinguish the broadening associated with self-

interaction from that due to environmental oxygen (Halpern et al., 1990). The authors also report a 20-fold increase in the sensitivity of the EPR spectrum to oxygen exchange broadening.

The spin label Tempone (spin label IV, Fig. 1) is one of the few nitroxide spin labels that shows no resolved proton coupling, and possesses a very narrow EPR line (0.25) G when dissolved at low concentration in a deoxygenated water solution. Narrower lines of 0.15 G can be obtained with deuteration of this spin label. Tempone has been used to measure oxygen consumption in biochemical reactions (Reszka and Sealy, 1984; Bielec et al., 1986), to record fast changes of oxygen concentration during photosynthesis (Strzalka et al., 1986; 1990), and to monitor the intracellular oxygen concentration (Wood et al., 1989).

Recently, a new type of oxygen-sensitive EPR molecular probe, triaryl methyl radical (trityl) (structure V in Fig. 1), was introduced (Ardenkjaer-Larsen et al., 1998). Trityls offer the possibility of an order-of-magnitude improvement in the signal-to-noise ratio, spatial resolution, and physiological sensitivity for *in vivo* spectral-spatial EPR imaging because of their very narrow linewidth (in the absence of oxygen it is approximately 25 mG). Images (with two spatial dimensions) of a mouse tumor were presented using this new type of stable free radical (Halpern et al., 1998).

2.2.2 Microscopic Spin-Label Probes

As can be seen from the Smoluchowski equation, the effect of molecular oxygen on EPR spectral characteristics of soluble oxygen-sensitive molecules depends on the diffusion-concentration product of oxygen in the solvent surrounding them. If they are dissolved in solvents with high oxygen solubility and high oxygen diffusion coefficients, they will be more sensitive to changes in oxygen tension. Hydrocarbons like paraffin oil or hexane are solvents which dissolve oxygen 4 - 10 times more than water (Linke, 1965), while the diffusion of oxygen is about as fast as in water (Subczynski and Hyde, 1984). The idea of having spin labels always surrounded by such solvents has been exploited in the oxygen-sensitive microscopic spin-label approach. Typical examples of microscopic spin-label probes are BSA-coated paraffin oil particles containing cholestane spin labels (Ligeza et al., 1992, 1994), or BSA-coated hexane particles containing stearic acid spin labels (Liu et al., 1994). Using such probes, it is possible to isolate nitroxides from water-soluble reductants and paramagnetic ions that might interfere with spin-label oximetry measurements. In these particles, the same hydrocarbon solvent that dissolves oxygen very well always surrounds spin label molecules. Therefore, the partial pressure of oxygen is the only factor that can influence the EPR spectrum of spin labels in the

microscopic probe. Such microscopic probes (a few micrometers in diameter) are readily and uniformly distributed within the sample, thus giving a rapid response to changes in oxygen partial pressure. For the purpose of protection against diffusion out of the liposome, liposomes containing the charged water soluble spin label 4-trimethylamonium-2,2,6,6,-tetramethylpiperidine-1-oxyl (Cat 1) were also used as a microscopic probe (Chan et al., 1989; Glockner et al., 1991).

2.2.3 Macroscopic Spin-Label Probes

The idea described above of enhancing the spin-label response to changes in oxygen partial pressure and isolating the spin-label solution from chemical and paramagnetic interference was used even earlier by Lukiewicz et al., who introduced macroscopic spin-label probes for *in vivo* oximetry measurements in 1984. The first experiments involved perdeutero ^{15}N Tempone solution in light paraffin oil, injected into the peritoneal cavity of a mouse (Fig. 3A). However, the spin label leaked out of the oil drop into the aqueous environment of the mouse body. To protect the spin label from leaking, the paraffin oil solution was enclosed in a gas-permeable TPX capsule before being placed in the peritoneal cavity of a mouse (Fig. 3B). *In vivo* oximetry measurements were performed at L-band using an EPR spectrometer with a loop-gap resonator (Subczynski et al., 1986). This method was further developed, and then used to measure the steady-state concentration of oxygen in solid tumors, which is critical for radiation therapy and experimental oncology (Lukiewicz, 1985).

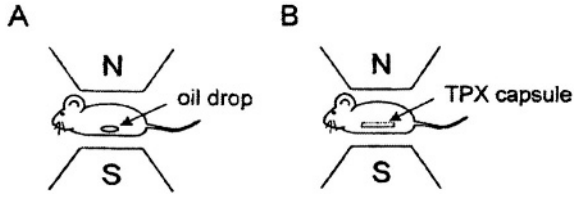

Figure 3. Diagram illustration of *in vivo* oximetry measurements. Mice (2-3 weeks old, weight approx. 20 g) were inserted into a cylinder of an L-band loop-gap resonator 25 mm in diameter and 30 mm long. An oil drop containing ^{15}N Tempone was injected into the peritoneal cavity of the animal (A). The TPX capsule containing a paraffin-oil solution of ^{15}N Tempone positioned in the peritoneal cavity of the animal (B).

2.2.4 Oximetry Based on Particulates

This approach uses insoluble, particulate materials based on carbonaceous materials (coals, charcoals, or India ink) or certain crystalline forms of lithium phthalocyanine (LiPc). These materials have EPR lines that are very sensitive to the presence of oxygen, often broadening several fold more in magnitude than the soluble materials used for EPR spin label oximetry. The mechanisms for the broadening can be quite complex and have been considered recently in detail in a review (Swartz and Clarkson, 1998). While used principally for measurements *in vivo* (Swartz, 2003), these probes also have been used for measurement of oxygen partial pressure in intact leaves (Ligeza et al., 1997) and in cellular systems (James et al, 1997; Vahidi et al., 1994).

2.3 Averaged and Local Oximetry Measurements

In the molecular probe method, spin label molecules are distributed more or less uniformly throughout the sample. Since the probe samples the fluid uniformly, the experimental parameter is proportional to the integral of the concentration over the sample volume - an important point if there is any reason to believe that oxygen gradients are present. If the sample being investigated is a homogenous fluid, the average oxygen concentration is easily determined using, for example, CTPO as a spin probe (Lai et al., 1982). If a molecular probe is applied to measure oxygen concentration in complex systems such as cells, the interpretation of the EPR data may be only qualitative. In such a system, the spin probes may not be uniformly distributed, and oxygen concentration can differ from place to place, and the oxygen diffusion coefficient can be different in different parts of the sample. Some of these difficulties can be avoided if the microscopic probe method is used. In this method the same solvent always surrounds label molecules, so the changes in the EPR spectrum are only related to the changes in oxygen partial pressure around the microscopic probe. This is schematically illustrated in Fig. 4 for a cell that is in equilibrium with a set percentage of air in the air/nitrogen mixture. Microscopic probes can easily be taken into the cell by phagocytosis, as was shown for BSA-coated paraffin droplets by Ito et al. (1981), who used them to study the phagocytic process of mouse peritoneal macrophages.

The approaches described above measure oxygen concentration and/or oxygen partial pressure averaged throughout the sample. However, if the spin-label molecule can be attached to a specific site of a protein or placed at a certain depth in the membrane, local oximetry measurement is possible. Measurement of oxygen accessibility to a certain spin-labelled amino acid is

necessary for depth-determination in site-directed spin labeling (SDSL) (Feix and Klug, 1998). Local oximetry measurements in the membrane are necessary for obtaining profiles of the oxygen diffusion-concentration product across the membrane, evaluation of the membrane permeability coefficient for oxygen, and discrimination of membrane domains. This subject will be discussed later in this chapter.

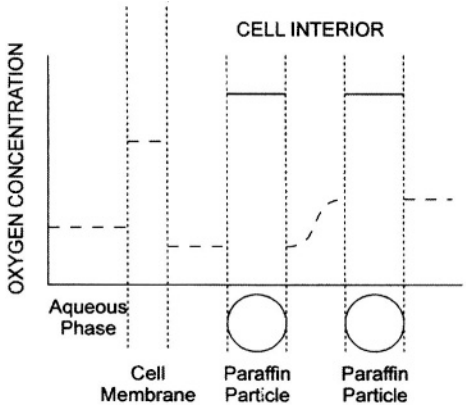

Figure 4. Schematic illustration of the local oxygen concentration sensed in the cell by molecular probes (- - - - -) and microscopic probes (---------) for the system in equilibrium with the set oxygen partial pressure (partial pressure of oxygen across the system is the same). The molecular probes measure the local (real) oxygen concentration which can significantly vary throughout the system (broken line). The concentration of oxygen inside the microscopic probes (paraffin particles containing a spin label) is the same, reflecting the partial pressure of oxygen with which the system was equilibrated. In this illustration oxygen consumption within the cell is neglected.

2.4 Oxygen Concentration, Partial Pressure, and Tension

Oxygen concentration, partial pressure of oxygen, and oxygen tension are mutually related values that, in principle, can be derived from one another. Oxygen concentration is expressed in moles per liter and is used for oxygen (solute) dissolved in bulk solvents. We can also talk about the local oxygen concentration in a certain region of the model and biological sample. Partial pressure of oxygen (torr or mm Hg) reflects the amount of oxygen in gas mixture and equals the pressure that oxygen would exert if it occupied the space by itself. For systems in equilibrium, the oxygen concentration in solution is determined exactly by the partial pressure of oxygen and the

solubility coefficient. For example, the concentration of oxygen in water saturated with air at 37°C (air contains 20.95% oxygen, which corresponds to a partial pressure of 159 mmHg, if the total pressure of air is one atmosphere) equals 220 μM. Oxygen tension is used mainly to describe oxygen concentration in systems that are not in equilibrium with gas phase (and usually not in equilibrium at all), like the human or animal body. It describes the very local oxygen concentration and is equal to the partial pressure of oxygen (the same units, torr or mm Hg) which, for system in local equilibrium, will give that certain local oxygen concentration.

In all EPR approaches described above the immediately measured value is the partial pressure of oxygen because for all oxygen sensitive paramagnetic materials, calibration curves can be produced that relate the observed EPR spectral parameter with the partial pressure of oxygen with which the probe is equilibrated (independently of the location of the probe: in gaseous phase, in a given solution, or in more complex environment). These calibration curves were produced for the molecular spin-label probe CTPO by saturating the CTPO water solution with a given oxygen/nitrogen mixture (with a given partial pressure of oxygen) and measuring the K parameter (Lai et al., 1982). They were produced for microscopic spin-label probes, BSA-coated paraffin oil particles, (Ligeza et al., 1992; 1994), as well as for particulate materials, coal derivative particles – fusinite (Ligeza et al., 1997). Also, EPR spectral parameter of a macroscopic spin probe, a TPX capsule containing ^{15}N Tempone solution in paraffin oil, was calibrated as a function of the partial pressure of oxygen (Subczynski et al., 1986).

Most often the molecular spin-label probe is dissolved in water for use in cell suspensions or for chemical reactions. In those cases the partial pressure of oxygen describes exactly the oxygen concentration in water phase (at a given temperature) and the calibration curves can be expressed as a function of oxygen concentration. These types of measurements (changing of oxygen concentration) were performed for measurements of oxygen consumption in CHO cell suspensions using CTPO (Lai et al., 1982; Ligeza et al., 1992) and in liposome suspension for measurement of lipid peroxidation (Subczynski and Kusumi, 1985; Kalyanaraman et al., 1987). The spin probe Tempone also was used for measurements of oxygen consumption (changing of oxygen concentration) in photo induced chemical reactions (Reszka and Sealy, 1984). Often, it is assumed that the environment surrounding the EPR probe is very similar to pure water and final data are expressed in concentration units. This was done for the microscopic spin-label probe (Ligeza et al., 1994), and for particulate materials (fusinite) (Ligeza et al., 1997) injected into the intact leaf as well as for a macroscopic spin-label probe implanted in the peritoneal cavity of a mouse (Subczynski et al., 1986). These assumptions, however, should be carefully justified.

Oxygen tension in tumors and different parts of animal body have been measured with the particulate oxygen sensitive paramagnetic materials such as coals, charcoals, India ink, or certain crystalline forms of lithium phthalocyanine. After placing one or more deposits of oxygen sensitive paramagnetic materials at sites of interest in rodents and then making repeated measurements only oxygen tension can be evaluated because surrounding tissue has no uniform structure and uniform solubility of oxygen (see section 7. OXIMETRY *IN VIVO* for more details). It is the local oxygen tension (local partial pressure of oxygen) in the very close vicinity of the particulate materials that is measured. These data cannot be transformed to concentration because at the same oxygen tension (oxygen partial pressure) oxygen solubility in different parts of tissue (cytoplasm, membranes) is different. It should be pointed here that the driving force for oxygen flow is not the difference in oxygen concentration but difference in partial pressure of oxygen (oxygen tension). Fig. 4 illustrates this situation in which for the system in equilibrium (oxygen consumption inside the cell is inhibited or neglected) the partial pressure of oxygen is the same in all points in the system but the local oxygen concentrations differ significantly. In this system net oxygen transport between different regions does not occur.

3. MEASUREMENTS IN CELL SUSPENSIONS

In early papers, the spin-label oximetry method was applied to measure the oxygen consumption rate in cell suspensions (Backer et al., 1977; Pajak et al., 1980; Sarna et al., 1980; Lai et al., 1982; see also reviews Swartz and Glockner, 1989; and Hyde and Subczynski, 1989). The closed-chamber approach was used in all of these measurements. In the closed-chamber method, cells are sealed into a gas-tight sample tube, enabling measurement of the rate of oxygen consumption by following the total concentration of oxygen in the sample. However, for studies seeking to determine oxygen concentrations in biological systems, an open-chamber approach usually is used. The open-chamber method offers the advantage of avoiding changes in oxygen concentration during an experiment. In this method, oxygen diffuses from the gas phase to the liquid phase in which it is used by the cells during respiration. Under steady-state conditions, the total respiration rate equals the rate at which oxygen diffuses into the sample. Typically, thin-walled capillaries made of gas permeable plastics such as Teflon (Plachy and Windrem, 1977) or the methyl pentene polymer TPX (Popp and Hyde, 1981; Subczynski and Hyde, 1981) have been used in EPR open-chamber measurements. This was the approach used by Swartz and collaborators in a series of studies that indicated that substantial gradients of oxygen

concentrations can occur across cell plasma membranes (Glockner et al., 1989; Hu et al., 1992).

Measurement of oxygen concentration in cell suspensions using EPR spin-label oximetry methods requires a relatively small sample volume, usually about 200 microliters (Lai et al., 1982). In some EPR approaches, the volume can be as small as 1 microliter (Froncisz et al., 1985). However, the concentration of cells has to be high, about 10^6-10^7 cells/ml for the closed-chamber approach (Lai et al., 1982) and 10^7 - 10^8 cells/ml for the open-chamber approach (Chan et al., 1989; Glockner et al., 1989, 1993; Hu et al., 1992). In the closed-chamber approach, the molecular spin-label probe is usually charged so that it is selectively located in the aqueous phase and does not penetrate into the cells. To measure the intracellular oxygen concentration directly, the EPR signal coming from molecular probes outside the cells has to be selectively suppressed. This is usually accomplished by using line-broadening agents such as $K_3Fe(CN)_6$ or potassium tris(oxalato) chromate III (CrOX), which do not penetrate the cell plasma membrane. These need to be used at fairly high concentrations (20 - 100 mM) so that the only visible EPR signal is from spin labels inside the cells.

3.1 Closed-Chamber Measurements

The measurements described below (Ligeza et al., 1994) basically repeat those made by Lai et al. (1982), using a much higher cell suspension density and paying attention not only to the oxygen concentration but also to the amplitude of the EPR spectrum of CTPO. The results are presented in Fig. 5. Fig. 5C shows that even at a cell suspension of 3×10^6 cells/ml, oxygen consumption is so rapid that it is difficult to measure its consumption rate. The integrated intensity of the EPR signal, which reflects the concentration of spin label remains essentially constant during these measurements. However, most often the EPR signal amplitude is recorded during this type of experiment. The increase in the signal amplitude at the beginning of the measurements is the result of the EPR line narrowing when oxygen is removed from the sample. This can be seen in Fig. 2 for the EPR signal of CTPO in a water solution equilibrated with air and nitrogen. For higher cell densities, a rapid decrease in the signal amplitude is also observed under these conditions, and the oxygen concentration drops to zero almost immediately after enclosing the sample in the Pasteur pipette. For a cell density of 50×10^6 cells/ml, the signal drops to 20% of its initial intensity during the first hour (Fig. 5A). The signal can be almost completely restored with $K_3Fe(CN)_6$, which indicates that the spin label has been reduced to its hydroxylamine. Swartz et al. (1986) reported that the rate of reduction of

some nitroxides in cell suspensions dramatically increased in anaerobic conditions. This suggests that nitroxides can be used as electron acceptors in cells.

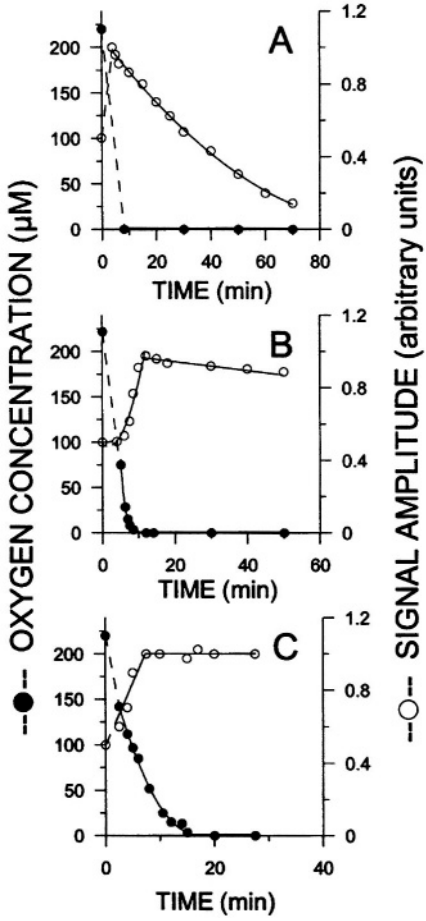

Figure 5. Kinetics of oxygen consumption by CHO cells in Earle medium at 37°C in a closed-chamber system for different cell densities (--●--): (A) 50×10^6 cells/ml, (B) 6×10^6 cells/ml, (C) 3×10^6 cells/ml. Kinetics of the changes of the EPR signal amplitude of CTPO during time course of oxygen consumption (--○--). Broken lines indicate kinetics between the sample preparation (air saturated samples) and beginning of the EPR measurements (adapted from Ligeza et al., 1994, with permission from Current Topics in Biophysics).

3.2 Open-Chamber Measurements

In the measurements described below (Ligeza et al., 1994) high density CHO cell suspensions enclosed in a TPX capillary and containing CTPO as an oxygen-sensitive molecular probe were used. Conditions were similar to those used for oxygen gradient measurements (Chan et al., 1989; Glockner et al., 1989, 1993; Hu et al., 1992). The oxygen flow through the plastic capillary wall from the gas around it to the cell suspension depends on the oxygen permeability coefficient of the plastic wall, and is proportional to the difference of oxygen partial pressure outside and inside the capillary (in the sample, just close to the capillary wall). Inside the capillary, in the liquid sample, diffusion is the only mechanism of oxygen transport (no stirring is applied). Oxygen is consumed constantly by cells distributed uniformly inside the capillary. To prevent or reduce cell sedimentation, the final medium contained 0.2 % methyl cellulose E4M (Dow), which is preferable to agar (0.1 %), which exhibits a tendency to aggregate in the sample tube. Oxygen consumption was not affected by this addition (Lai et al., 1982).

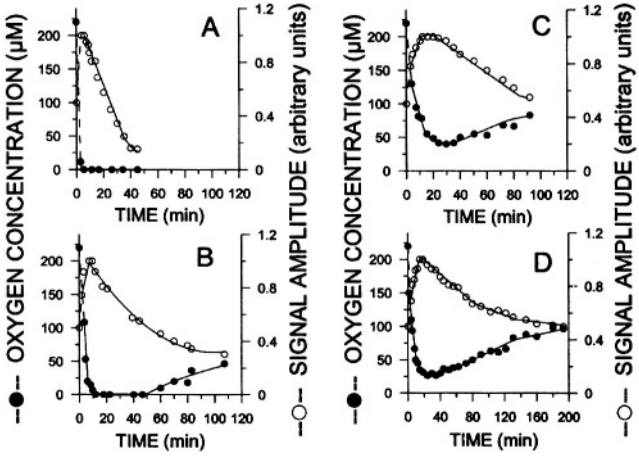

Figure 6. Changes in oxygen concentration in a CHO cell suspension in Earle medium (A, B, C) and Hanks medium (D) at 37°C in an open-chamber system for different cell densities (--●--): (A) 60×10^6 cells/ml, (B) 20×10^6 cells/ml, (C) 10×10^6 cells/ml, (D) 10×10^6 cells/ml. Kinetics of the changes in the EPR signal amplitude of CTPO during the time course of oxygen consumption (--○--). Inside the EPR cavity, the system was continuously equilibrated with a gas mixture of 47.5% air, 47.5% nitrogen and 5% carbon dioxide. Before positioning inside the cavity, the sample was equilibrated with air. Broken lines indicate kinetics between the sample preparation and beginning of the EPR measurements (adapted from Ligeza et al., 1994, with permission from Current Topics in Biophysics).

The results for different densities of cell suspensions are presented in Fig. 6. Several features are especially notable: (1) For higher cell densities (60×10^6 cells/ml), oxygen concentration dropped to zero in about five minutes and stayed at that level during further measurements (about 40 minutes) (Fig. 6A), while at lower cell densities (20×10^6 cells/ml), oxygen concentration dropped to zero after about 10 minutes. After about 50 minutes, it started to increase again to a fairly high level (~50 μM after 100 minutes) (Fig. 6B). (2) At a cell density of $10x\times10^6$ cells/ml, the oxygen concentration dropped to its minimum value of ~30 μM after about 25 minutes, but started to increase again, reaching 100 μM (practically the concentration in equilibrium with the gas outside the capillary, which contains 47.5% air) after 3 hours (Fig. 6C and 6D). (3) Significant spin label reduction was observed after the concentration of oxygen dropped to zero or reached a minimum. (4) The rate of spin label reduction was roughly proportional to the density of cell suspension.

These results raised at least two questions: (1) Why, after reaching the minimum (or zero) level, did the oxygen concentration increase again? (2) Why was the spin label reduced in the aerated sample? The answer may be found, at least in part, in a quantitative evaluation of some of the variables.

3.2.1 Pool of Substrates for Cell Respiration

D-glucose is the major source of energy for CHO cells suspended in an Earle or Hanks media. In the cell, oxygen is consumed mainly during respiration and this process can be summarized as follows:

$$C_6H_{12}O_6 + 6O_2 \rightarrow 6CO_2 + 6H_2O + \text{Energy} \qquad (4)$$

How long can the medium provide substrates for cell respiration? Both Earle and Hanks media contain 1 g of glucose/l. A simple calculation shows that for a cell density of 10^8 cells/ml, glucose will be exhausted after 90 minutes, assuming that all cells are working with the maximum respiration rate ($V = 6\times10^{-17}$ moles O_2/(s×cell); Lai et al., 1982). This calculation shows that respiratory substrates are in substantial excess in the medium; therefore, the increase in oxygen concentration observed in open-chamber measurements cannot be explained by the lack of substrates. Another potential factor is the accumulation of products of cell metabolism that are not removed using the open-chamber system. This may be a cause of the apparent change in cell metabolism, which is indicated by an increase in spin-label reduction and decrease in the rate of oxygen consumption by the cells (Fig. 6).

3.2.2 Profile of Oxygen Concentration Inside the Open Chamber

Inside the oxygen-permeable capillary, oxygen diffuses from the wall to the capillary center through the suspension of respiring cells. After the system reaches equilibrium, a steady oxygen concentration profile is created inside the capillary. Boag (1969) gives the expressions for the spatial profile of oxygen concentration for the penetration of oxygen into a cylinder of metabolizing tissue (capillary with metabolizing cell suspension in the case described here), assuming that the rate of oxygen consumption is uniform inside the cylinder and independent of oxygen concentration. These conditions were fulfilled in the described experiment: the cells were uniformly distributed and the rate of oxygen consumption remained constant to a very low oxygen concentration (Lai et al., 1982; Froncisz et al., 1985). There are two distinct cases: (1) if the radius R of the capillary is large enough, the oxygen concentration reaches zero at $r = a$ ($C_{r=a} = 0$) and remains zero for $r < a$, and (2) the oxygen concentration on the axis $r = 0$ is $C_{r=0} \geq 0$ (see Fig. 7). In the first case, the radius a is determined by the equation:

$$\frac{4C_R D_O}{\rho V R^2} = 1 - \frac{a^2}{R^2} - \frac{a^2}{R^2} \ln \frac{R^2}{a^2} \tag{5}$$

and the profile of oxygen concentration for $r > a$ is described by the equation:

$$C = \frac{(r^2/a^2) - 1 - 2\ln(r/a)}{(R^2/a^2) - a - 2\ln(R/a)} C_R. \tag{6}$$

In the second case, the profile of oxygen concentration is described by the equation:

$$C = C_R - \frac{\rho V}{4D_O}(R^2 - r^2). \tag{7}$$

The concentration in the capillary center at $r = 0$ is given by:

$$C_{r=0} = C_R - \frac{\rho V R^2}{4D_O}. \tag{8}$$

The radius of the capillary, R_o, for which the oxygen concentration just falls to zero in the capillary center equals:

$$R_O = \sqrt{4D_O C_R / \rho V}. \tag{9}$$

In these equations, C_R is the oxygen concentration just at the inner wall of the capillary (at radius R). V is the oxygen consumption rate per cell, ρ is the cell density and D_O is the oxygen diffusion coefficient in the medium.

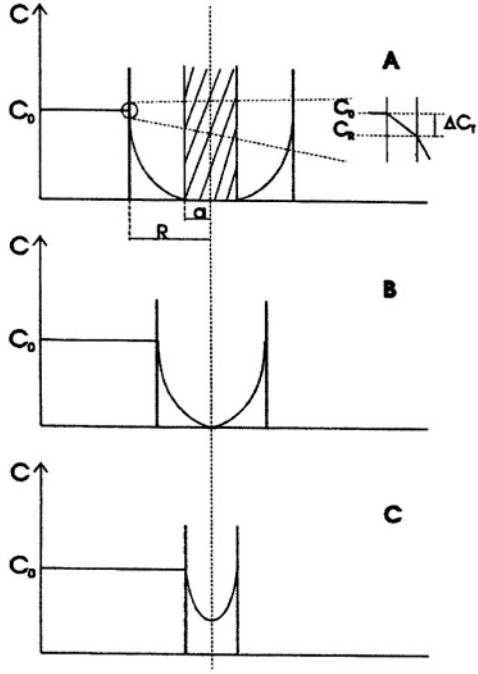

Figure 7. Profiles of the oxygen concentration (C) inside open-chamber capillaries with different capillary diameters and containing cell suspensions with the same cell densities. (A) For the large diameter (2R), the oxygen concentration drops to zero at the radius *a.* Cross-hatched area indicates cells in anoxic conditions. (B) For this dimension, the oxygen concentration drops to zero at the capillary center. (C) At all sites, the oxygen concentration is greater than zero. Insert in Fig 7A indicates the drop in oxygen concentration across the capillary wall (ΔC_T) from C_O (the concentration of oxygen in water equilibrated with the gas outside the capillary) to C_R (the concentration of oxygen in cell suspension just at the inner capillary surface) (from Ligeza et al., 1994, with permission from Current Topics in Biophysics).

Let us assume that outside the capillary there is pure air and that the oxygen partial pressure difference across the capillary wall equals zero. In that case, the radius R_o obtained from Eq. 9 is $R_o = 0.6$ mm for the capillary filled with the CHO cell suspension of density $\rho = 10^8$ cells/ml (consuming oxygen at 37°C with a rate $V = 6\times10^{-17}$ moles O_2/(s×cell) (Lai et al., 1982)). At this temperature, the oxygen diffusion coefficient in water is $D_O = 3\times10^{-5}$ cm^2/s (St. Denis and Fell, 1971) and the oxygen concentration for water equilibrated with air $C_R = 220$ μM (Hitchman, 1978]). This cell density is

often used in open-chamber measurements (Chan et al., 1989; Glockner et al., 1989, 1993; Hu et al., 1992).

The experiments described above used a TPX capillary of R = 0.35 mm, a gas mixture outside the capillary containing 47.5% air (C_R = 105 μM), and maximal and minimal cell densities of 6×10^7 and 10^7 cells/ml respectively. According to Eq. (8), the oxygen concentration in the capillary center for these samples drops to the value $C_{r=0}$ = 63 μM and 98 μM, respectively. In these evaluations, it was assumed that the drop of oxygen partial pressure across the capillary wall is zero. It was shown experimentally that after the change of the gas outside this TPX capillary at 37°C from air to nitrogen, the oxygen concentration in the water sample inside the capillary drops by a factor of e during 1.5 min. Knowledge of this characteristic time allowed for evaluation of the permeability coefficient of the TPX wall as 21 (μM O_2/atm)×(cm/s). Assuming that all CHO cells were respiring at the maximum rate, the oxygen partial pressure difference across the TPX capillary wall for cell densities of 10^7, 3×10^7 and 6×10^7 cells/ml equals 0.05, 0.1 and 0.3 atm, respectively. These can be related to the difference of oxygen concentration in water of 55, 110, and 330 μM, respectively.

These calculations correlate well with the results presented in Fig. 6. The drop in oxygen concentration across the TPX wall (65 - 75 μM) for a cell density of 10^7 cells/ml is comparable to the evaluated value of 55 μM (Fig. 6C and 6D). For higher cell densities, oxygen concentration drops to zero (Figs. 6A and 6B). As can be seen from these evaluations, there are four parameters which characterize the cell suspension and the open-chamber capillary which are critical – cell density, cell respiration rate, radius of the capillary and permeability of the capillary wall to oxygen. The following conclusions can be made: (1) Spin-label reduction is not significant during the timespan of the experiments in the closed-chamber system, presumably because the experiment is concluded before the oxygen is exhausted. (2) Substrates for cell respiration are not exhausted in closed-chamber experiments. (3) The oxygen consumption rate of the cells is not constant during the timespan of the experiment in the open-chamber system, and that is manifested by the later increase in oxygen concentration in the sample. (4) The decrease in the oxygen consumption rate occurs much earlier than exhaustion of the substrates for cell respiration. (5) The decrease in the oxygen consumption rate is accompanied by significant spin-label reduction. (6) For dense cell suspensions, a significant oxygen partial pressure difference across the capillary wall can be created. (7) For dense cell suspensions, the decrease in oxygen concentration from the capillary wall to its center can be as great as 100 - 200 μM. (8) Therefore, it is possible that for cells with a high respiration rate, the cells located near the center of the

capillary will be anoxic. These consideration should be taken into account during measurements with an open-chamber system.

4. OXYGEN SOLUBILITY AND DIFFUSION IN LIPID BILAYER MEMBRANES

The most important parameter in understanding chemical reactions involving oxygen is the product of its local diffusion coefficient and local concentration. This product is of fundamental interest in itself, and separation into its component factors (the diffusion coefficient and concentration) is not necessary. Spin-label oximetry allows measurement of this product in restricted domains such as membranes, or more accurately, at a certain depth in membranes. For oxygen, the important chemical reactions that occur within the membrane include lipid peroxidation and the formation of reactive oxygen species. Recently, the reaction of NO with oxygen within the lipid bilayer membrane attracted the attention of researchers (Singh et al., 1994; Stamler, 1995). It was shown that in the hydrophobic environment of a model or biological membrane, this reaction is approximately 300 times faster than in water (Liu et al., 1998). Hydrophobic compartments of the cell should therefore be considered to be important sites of NO disappearance. For these types of reactions spin-label oximetry and spin-label NO-metry (Subczynski et al., 1996; Lomnicka and Subczynski, 1996; Subczynski and Hyde, 1998b) can give the basic data on oxygen and NO local diffusion-concentration product. We will refrain from discussing chemical reactions involving molecular oxygen any further.

Spin-label oximetry makes it possible to measure the transport of oxygen both within and across the lipid bilayer model membrane and in the lipid portion of biological membranes (Kusumi et al., 1982; Subczynski et al., 1989). This approach was used to obtain profiles of the oxygen diffusion-concentration product across the membrane. Knowledge of these profiles makes it possible to evaluate the membrane oxygen permeability coefficient (Subczynski et al., 1989). In these types of experiments, samples (spin-labeled liposomes or biological membrane suspensions) should be precisely equilibrated with the given partial pressure of oxygen at a defined temperature. This is possible with the use of TPX gas permeable capillaries (Popp and Hyde, 1981; Subczynski and Hyde, 1981; Hyde and Subczynski, 1989). The importance of the TPX gas-exchanging sample cell to the development of spin-label oximetry and its application in membranous systems has been very great.

4.1 Oxygen Transport Parameter

If it is possible to put a spin label in restricted domains such as a membrane, its bimolecular collision frequency with oxygen in this specific environment can be recorded. In the T_1-sensitive methodology applied to lipid bilayer membranes, the bimolecular collision rate is evaluated in terms of an oxygen transport parameter using a saturation recovery EPR technique (Kusumi et al., 1982; Subczynski et al., 1989, 1991a). Previously, the notation used for the oxygen transport parameter was $W(x)$ (Kusumi et al., 1982: Subczynski et al., 1989, 1991a, 1992a, 1998; Ashikawa et al., 1994). However, in the paper by Kawasaki et al. (2001), this was changed to $2P(x)$ because different W values were used to indicate electron spin transition rates. In this review, $2P(x)$ will be used for the oxygen transport parameter as well. $2P(x)$ at location x in the membrane is defined as

$$2P(x) = T_1^{-1}(x, \text{air}) - T_1^{-1}(x, N_2) \tag{10}$$

where the T_1s are the spin-lattice relaxation times of the nitroxide in samples equilibrated with atmospheric air and nitrogen, respectively. According to the Smoluchowski equation (Eq. 3), the collision rate is thus proportional to the product of the local translational diffusion coefficient of oxygen $D_O(x)$ and the local oxygen concentration $C_O(x)$ in a membrane equilibrated with atmospheric air

$$2P(x) = AD_O(x)C_O(x), \qquad A = 8\pi p r_o \tag{11}$$

As noted, p is close to one (Hyde and Subczynski, 1989). In this equation, x indicates the different depths in the membrane at which EPR measurements were performed. These measurements can be easily done by attaching the nitroxide moiety to different carbon atoms of the hydrocarbon chain in stearic acid or phosphatidylcholine molecules, or to their polar head groups (see scheme in Fig. 8). Note that $2P(x)$ is a value extrapolated to a sample equilibrated with 100% air and that $C(x)$ is proportional to the oxygen partial pressure in the equilibrating gas mixture.

Profiles of the oxygen transport parameter across the membrane allow one to understand the movement of oxygen molecules within the lipid bilayer membranes and calculate the oxygen permeability coefficient across model and biological membranes (Subczynski et al., 1989, 1991a, 1992a; Subczynski and Markowska, 1992; Ashikawa et al., 1994; Ligeza et al., 1998; Marsh, 2001). The fluid-phase model and biological membranes show similar bell-shaped profiles of $2P(x)$, with the oxygen diffusion-concentration product in the membrane center being a few times greater than that in or near the head group region. The typical profile of the oxygen transport parameter $2P(x)$ across the 1-palmitoyl-2-oleoylphosphatidylcholine (POPC) bilayer obtained with the use of

phospholipid spin labels is shown in Fig. 9. Profiles of the product of oxygen diffusion-concentration across the lipid bilayer membranes can be also obtained using the linewidth (T_2) method as was shown by Smirnov et al. (1996)

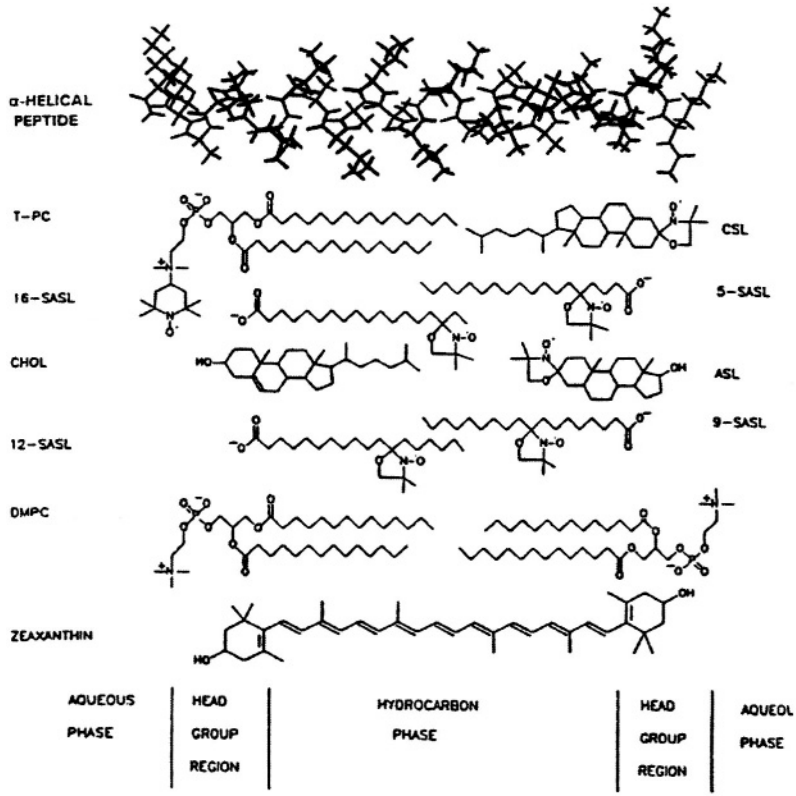

Figure 8. Cross-section of the DMPC membrane including membrane modifiers (cholesterol, CHOL), polar carotenoid - zeaxanthin, and transmembrane α-helical peptide – Ac-$K_2(LA)_{12}K_2$-amide) and lipid spin labels. Locations across the membrane are illustrated.

4.2 Oxygen Membrane Permeability Coefficient

One of the most fundamental properties of biological membranes is that they are barriers to the permeation of polar molecules. This is largely due to the hydrophobicity of the membrane interior. However, it cannot be automatically applied to the permeation of small solutes such as oxygen and nitric oxide, even though some experimental data suggest this to be true (Nicholson and Roughton, 1951; Holland, 1967; Chan et al., 1989; Glockner et al., 1989, 1993; Hu et al., 1992; Vaughn et al., 2001). It is practically

impossible to measure the membrane permeability of oxygen directly by the creation of fast decaying gradients. There is, however, another approach in which oxygen transport parameter profiles across the membrane, obtained for samples in equilibrium with oxygen and nitrogen (without creating any fast decaying oxygen gradients), are used to calculate the permeability coefficient (Subczynski et al., 1989). The membrane permeability coefficient, P_M, is a useful physical characteristic of a membrane as a whole which connects the oxygen flux across the membrane, J, with the difference in oxygen concentration in the aqueous phase on either side of the membrane (C''- C'):

$$J = -P_M(C'' - C') \tag{12}$$

P_M can be calculated from the $2P(x)$ profiles on the basis of Diamond and Katz's theory (1974) developed for permeability of nonelectrolytes, according to the procedure developed by Subczynski et al. (1989). In this approach, it is necessary to make an integration of $(D_O(x)C_O(x))^{-1}$, which is a measure of the resistance of the membrane to oxygen transport over its entire thickness, h. The product $(D_O(x)C_O(x))^{-1}$ can be related to the oxygen transport parameter through Eqs. 10 and 11. The final equation for the membrane permeability coefficient, which is based on the oxygen transport parameter profiles, as that shown in Fig. 9, has the form (Subczynski et al., 1989):

$$P_M = \frac{1}{AC_o(\text{water})}\left[\int_0^h \frac{dx}{2P(x)}\right]^{-1} \tag{13}$$

Here, $C_O(\text{water})$ is the oxygen concentration in the aqueous phase equilibrated with air. However, the uncertainty of A $(=8\pi pr_o)$ in Eq. (11) could lead to a possible error. Fortunately, since A is remarkably independent of solvent viscosity, temperature, hydrophobicity and spin-label species (Hyde and Subczynski, 1984, 1989; Subczynski and Hyde, 1984), the ratio of the permeability coefficient across the membrane, P_M, to the permeability of the water layer of the same thickness, h, as the membrane, P_W, obtained using the same EPR method, can cancel this error. The oxygen permeability of a water layer of thickness h equals:

$$P_W = \frac{1}{AC_o(\text{water})}\left[\frac{h}{2P(\text{water})}\right]^{-1}. \tag{14}$$

The oxygen transport parameter in water, $2P$(water), can be measured using water soluble spin label d-Tempone (Subczynski et al., 1989, 1991a, 1992a). Using T_1 measurements in membranes and in water, the ratio of P_M(pulse EPR)/P_W(pulse EPR) can be determined. The permeability coefficient of oxygen in a water layer of thickness h, can also be determined from the macroscopic oxygen diffusion coefficient in bulk water, D_O(water) (St. Denis and Fell, 1971), according to the equation:

$$P_w = D_O(water)/h. \tag{15}$$

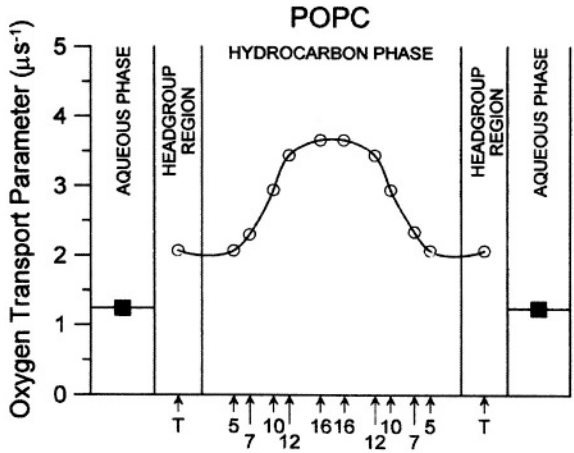

Figure 9. Profile of the oxygen transport parameter, $2P$(x), across the POPC bilayer obtained at 35°C with the n-PC spin labels (○). The oxygen transport parameter in the aqueous phase was obtained with d-Tempone, and is shown for comparison (■). Approximate locations of nitroxide moieties of spin labels are indicated by arrows.

The P_M (pulse EPR) value is evaluated using Eq. (13) with the integration performed based on figures such as Fig. 10 (top), where $(2P(x))^{-1}$ is plotted as a function of distance from the center of the membrane. The manner of integration of the oxygen permeability coefficient across a water layer of the same thickness as a membrane (Eq. 14) is shown in Fig. 10 (bottom). The ratio of P_M(pulse EPR)/P_W(pulse EPR) is simply the ratio of these two integrals. Using T_1 measurements in membranes and in water, the ratio of P_M(pulse EPR)/P_W(pulse EPR) can be determined, and using the value of P_W obtained from Eq. (15), we arrive at a value of the oxygen permeability coefficient across the membrane. Data for different membranes and conditions are collected in Table 1. The membrane oxygen permeability

coefficient can also be obtained using oxygen-induced EPR line-broadening measurements. For details see Subczynski and Markowska (1992) and Subczynski and Hyde (1998a, 1998b).

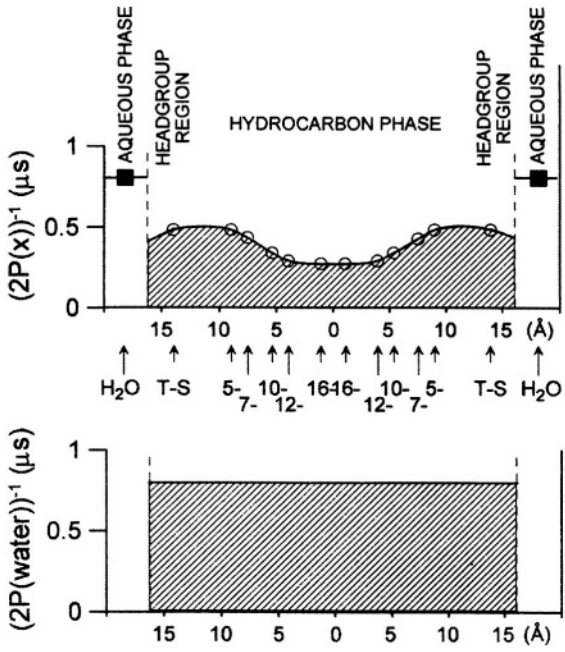

Figure 10. (Top) $(2P(x))^{-1}$ is plotted as a function of the distance from the center of the POPC (1-palmitoyl-2-oleoylphosphatidylcholine) membrane equilibrated with air at 35°C to show the oxygen permeability barriers and method of integration based on Eq. 13 (i. e., measuring the hatched area under the solid curve). The thickness of the membrane and positions of the nitroxide moieties are assumed to be the same as evaluated earlier for EYPC (egg yolk phosphatidylcholine) bilayer (Subczynski et al., 1989, 1991a). (Bottom) $(2P(water))^{-1}$ at 35°C plotted for the water layer of the same thickness as the membrane to illustrate the method of integration based on Eq. 14 (i. e., measuring the hatched area under the solid line).

Table 1. Oxygen permeability coefficients for different membranes.

Membrane	Temperature (°C)	P_M(cm s^{-1})	Reference
DMPC[a]	8	5.3	Subczynski et al., 1989
DMPC	25	105.0	Subczynski et al., 1992a
DMPC	38	185.0	Subczynski et al., 1989
DMPC–10% zeaxanthin	25	59.0	Subczynski et al., 1992[a]
DMPC–50% cholesterol	38	38.0	Subczynski et al., 1989
EYPC[b]	25	119.0	Subczynski et al., 1992a
EYPC	40	201.5	Subczynski et al., 1991
EYPC–10% zeaxanthin	25	88.0	Subczynski et al., 1992a
EYPC–50% cholesterol	40	73.4	Subczynski et al., 1991
CHO plasma membrane	37	42.0	Subczynski et al., 1992[b]
Thylakoid membrane	20	39.5	Ligeza et al., 1998
SLOT[c]	35	34.7	Ashikawa et al., 1994
Purple membrane	35	21.3	Ashikawa et al., 1994

[a]Gel-phase membrane
[b]Egg yolk phosphatidylcholine (EYPC) membrane
[c]Measurements for slow oxygen-transport domain in reconstituted membranes of BR and DMPC (BR/DMPC=1/40).

4.3 Effect of Membrane Modifiers in Model Membranes

4.3.1 Cholesterol

Membrane modifiers affect oxygen transport parameter profiles differently in different membrane regions. Cholesterol significantly decreases oxygen transport in the polar head group region and in the hydrocarbon region near the polar head groups, and increases it in the membrane center (Subczynski et al., 1989, 1991). Cholesterol affects the hydrophobicity profile across the phospholipid bilayer in a similar manner, increasing hydrophobicity in the membrane center and decreasing it in and near the polar head group region (Marsh and Watts, 1981; Subczynski et al., 1994; Marsh, 2001). It therefore can be assumed that the solubility (distribution of oxygen molecules within the lipid bilayer) makes a significant contribution to the cholesterol-induced changes in the oxygen transport parameter profile. Some resistance to oxygen permeability across the membrane is located in and near the head group region. In the center, oxygen transport parallel to the membrane surface seems to be more effective than the transport across the cytosol. As can be seen from Table 1, cholesterol at high concentration decreases the membrane permeability to oxygen in fluid-phase model membranes by a factor of 3 - 5.

4.3.2 Carotenoids

Polar carotenoids like lutein and zeaxanthin decrease the oxygen diffusion-concentration product in saturated and unsaturated membranes (Subczynski et al., 1991b). The effect is strongest in the membrane center and negligible in the head group region. At 10 mol%, polar carotenoids decrease the value of P_M of model membranes by a factor of 2 (Subczynski and Markowska, 1992). Polar carotenoids significantly increase the hydrophobicity of the membrane interior (Wisniewska and Subczynski, 1998), which suggests their strong effect on the oxygen translational diffusion coefficient rather than oxygen concentration within the lipid bilayer. The different effects of cholesterol and polar carotenoids on oxygen transport can result from different structures and different localization of these molecules in the membrane. The cholesterol molecule is located in one half of the bilayer, and its rigid plate-like portion extends to the depth of the 7^{th} to 10^{th} carbon atoms in lipid hydrocarbon chains (McIntosh, 1978). In contrast, one carotenoid molecule influences both halves of the lipid bilayer and, with two polar groups interacting with opposite hydrophilic surfaces of the membrane; it can brace together the two halves of the bilayer like a tie-bar (Rohmer et al., 1979). Therefore, the oxygen diffusion-concentration product is reduced in those regions of the bilayer to which the rigid portion of the molecule of the modifier extends (see scheme in Fig. 8).

4.3.3 Transmembrane α-Helical Peptides

Surprisingly, the transmembrane α-helical peptides of similar structures, L_{24} and $(LA)_{12}$ (Ac-$K_2L_{24}K_2$-amide and Ac-$K_2(LA)_{12}K_2$-amide, respectively), affect oxygen transport in the POPC bilayer in a strikingly different way (Subczynski et al., 1998, 2003). The effect of L_{24} is minimal in the membrane center and increases towards the head group region. $(LA)_{12}$ decreases oxygen transport very strongly across the entire lipid bilayer. The effect is strongest in the membrane center, where 10 mol% of $(LA)_{12}$ decreases this parameter by about 50% (as compared to no effect from L_{24}). Close to the polar head group, the 10 mole% of $(LA)_{12}$ decreases the oxygen transport parameter by 40%, compared to the 20% decrease caused by L_{24}. The much stronger effect of $(LA)_{12}$ is ascribed not only to the increased roughness of its hydrophobic surface but also to the increased motional freedom of its leucine side chains. In L_{24} the leucine side chains are packed tightly, giving a smooth hydrophobic surface. In $(LA)_{12}$ they are separated by the small methyl groups of the alanine side chains, giving them additional motional freedom and the ability to protrude between the phospholipid hydrocarbon chains. These differences are not detected by conventional

EPR spectra, showing once again that oxygen is more sensitive in detecting differences in the dynamic organization of the membrane. It can be speculated that the major effect of these peptides, $(LA)_{12}$ in particular, on the oxygen transport parameter is through the decrease of oxygen translational diffusion because both peptides increase the hydrophobicity across the POPC bilayer (Subczynski et al., 1998, 2002). Thus, a comparison of the effects of membrane modifiers on the oxygen transport parameter profile and the hydrophobicity profile across the lipid bilayer can help analyze which component of the oxygen diffusion-concentration product – diffusion coefficient or concentration – is primarily affected.

4.4 Biological Membranes

The spin-label oximetry approach allows for evaluation of the oxygen permeability coefficient only in the lipid-bilayer portion of biological membranes. Because of this, the overall (average) membrane permeability should be further corrected for the presence of integral membrane proteins. P_M values for biological membranes are listed also in Table 1. It was shown that the oxygen permeability coefficient measured in the lipid bilayer portion of the Chinese hamster ovary plasma membrane is about two times lower than that of an appropriate water layer (Subczynski et al., 1992a), while that of the thylakoid membrane is about the same as that of the water layer (Ligeza et al., 1998). The smallest P_M is observed for lipid domains crowded with integral membrane proteins. The lipid domain of the purple membrane isolated from *Halobacterium halobium* shows a P_M about 6 to 10 times smaller than that of the fluid-phase lipid bilayer (Ashikawa et al., 1994). To obtain a depth measurement using SDSL, calibration of the accessibility of different relaxation agents including oxygen (accessibility profiles) into the lipid bilayer of the given membrane is performed using n-PC (1-palmitoyl-2-(n-doxylstearoyl)phosphatidylcholine) spin labels and CW saturation measurements (Altenbach et al., 1994; Feix and Klug, 1998). The accessibility profiles cannot be directly related to the membrane oxygen permeability coefficient, but can show the ability of oxygen to penetrate into the lipid bilayer. These calibrations were also performed for biological membranes, e.g. rod outer segment disk membranes by Farahbakhsh et al. (1992), showing that this membrane is also easily penetrated by oxygen.

As has already been shown, oxygen transport across the membrane depends significantly on membrane constitution. Cholesterol at high concentrations significantly decreases oxygen transport across the lipid bilayer (Subczynski et al., 1989, 1991a). Here it must be noted that cholesterol is especially abundant in the plasma membrane of mammalian cells. Also, protein content in the membrane can affect oxygen permeability

in two ways. First, integral membrane proteins are practically impermeable to oxygen (Altenbach et al., 1990; Subczynski et al., 1992b). Because of that, the oxygen concentration difference across the membrane, evaluated on the basis of knowledge of the oxygen permeability coefficient of the lipid bilayer portion of the membrane, should be increased by a factor proportional to the surface area of the membrane divided by the surface area of its lipid bilayer portion. Second, integral membrane proteins affect the oxygen permeability of the lipid bilayer itself mainly by creating protein-rich domains with trapped lipids (Ashikawa et al., 1994) and/or cholesterol-rich raft domains stabilized by the presence of clustered proteins (Kawasaki et al., 2001). In the cholesterol-rich raft domain of the influenza viral (IFV) membrane, oxygen transport was decreased by a factor of 16 compared to bulk lipids (Kawasaki et al., 2001). These studies, however, introduce another level of complication that will be discussed in the next section.

The overall conclusion from this type of investigation is that biological membranes are not barriers to oxygen transport, and oxygen concentration differences across cell plasma membranes, even during intensive respiration, are negligible. Evaluations presented by Subczynski et al. (1991a) show that this difference is in the nanomolar range for cell and mitochondrial membranes. A membrane overloaded with cholesterol and integral proteins can be a barrier only if the cell or mitochondrion radius is very small, becoming comparable to the membrane thickness itself (Subczynski et al., 1992a).

5. DOT METHOD (METHOD OF DISCRIMINATION BY OXYGEN TRANSPORT)

Molecular oxygen as a membrane probe has certain unique characteristics: its small size and appropriate level of hydrophobicity allow it to enter the small vacant pockets transiently formed in lipid bilayer membranes. Because of this, the molecular collision rates between oxygen and nitroxide radical spin labels placed at specific locations in the membrane are sensitive to the dynamics of *gauche-trans* isomerization of lipid alkyl chains and to the structural nonconformability of neighboring lipids (Subczynski et al., 1991a). Thus, the three-dimensional dynamic structure of the lipid bilayer membrane can be investigated using the spin-label oximetry approach. The oxygen transport parameter was successfully used as a sensitive monitor of the membrane structure and dynamics because the effect of oxygen on the spin-lattice relaxation time of spin labels is generally much greater than the motional effects (Kusumi et al., 1982).

The DOT method (the method of discrimination by oxygen transport) developed by Ashikawa et al. (1994) was successfully used to indicate the existence of lipid domains in model and biological membranes with different oxygen transport parameters. In this type of measurement, the lipid spin label is located in the membrane domains with fast and slow oxygen transport. Because the DOT method is based on the measurements of T_1 of lipid spin labels in the absence and presence of oxygen, which ranges from 0.1 to 10 μs, the exchange rate of spin labels between these domains must be slower than or comparable to these times. If the exchange rate is faster, the oxygen collision rate cannot distinguish the existing domains. This was the case in the reconstituted membranes of bacteriorhodopsin (BR) and dimyristoylphosphatidylcholine (DMPC) for a low BR/lipid ratio (1/80) (Ashikawa et al., 1994). In the absence and presence of molecular oxygen (up to 50% of atmospheric air), only single exponential saturation-recovery curves were observed for lipid spin labels with the oxygen transport parameter about 1.5 times smaller than in a pure lipid bilayer. Because it is evident that the lipid bulk and lipid boundary regions around BR molecules coexist in this sample (East et al., 1985; Ryba et al., 1987; Horvath et al., 1988; Marsh, 1997), the exchange rate of lipids between the bulk and the boundary regions must be much faster than the time range of the method. Therefore, in the following sections, the bulk plus boundary regions will be indicated as the BULK domain for simplicity.

5.1 SLOT (Slow Oxygen Transport) Domains

In membranes consisting of two lipid environments with different oxygen transport rates (slow oxygen transport (SLOT) domain and fast oxygen transport (BULK) domain) and exchange rates of the spin-labeled lipids between these domains slower than 10^4 s^{-1}, the EPR saturation-recovery signal will be a simple double-exponential curve with time constants of $T_1^{-1}(f_{air}, \text{SLOT})$ and $T_1^{-1}(f_{air}, \text{BULK})$.

$$T_1^{-1}(f_{air}, \text{SLOT}) = 2P_1 f_{air} + T_1^{-1}(N_2, \text{SLOT}) \tag{16}$$

$$T_1^{-1}(f_{air}, \text{BULK}) = 2P_2 f_{air} + T_1^{-1}(N_2, \text{BULK}) \tag{17}$$

Here "x" in Eqs. (10) and (11) is changed to the two-membrane domain, BULK and SLOT, and the depth is fixed. The same lipid spin label is distributed between the BULK and SLOT domains. Because $C(x)$ is proportional to the partial pressure of oxygen in the equilibrating gas mixture, the fraction of air in the gas mixture, f_{air}, used in actual experiments is introduced. $2P_1$ and $2P_2$ are oxygen transport parameters in each domain.

Because these $2P$ values are the rates of collision between the spin label and molecular oxygen extrapolated to a sample equilibrated with 100% air, $2Pf_{air}$ represents the collision rate in a sample equilibrated with a gas containing f_{air} air. In general, $T_1^{-1}(N_2, SLOT)$ and $T_1^{-1}(N_2, BULK)$ are close in the membrane and the presence of two types of lipid domains often can be clearly manifested only after the introduction of molecular oxygen to the sample. The collision rate of molecular oxygen with the nitroxide group of the spin label can differ substantially between the two domains.

This approach allows for detecting the presence of a specific lipid domain that exhibits a slow oxygen transport rate. The SLOT domain was detected in BR reconstituted membranes at a BR/lipid ratio of 1/40, in which the oxygen transport rate was smaller by a factor of 5 than in the BULK region (Ashikawa et al., 1994). This domain is thought to be protein rich, in which every lipid molecule is in contact with two proteins or with protein and boundary lipids (thus the lipids are sandwiched either between two proteins or between a protein and boundary lipids) and its hydrocarbon chain motion is suppressed to the level of the gel-phase membrane. The exchange rate of lipids between this domain and the BULK domain has not been observed.

Recently, two different oxygen transport rates were detected in DMPC membranes containing 20 mol% cholesterol (Subczynski, preliminary results). As can be seen from Figs. 11A and 11B, a double (but not a single) exponential can be fitted to the saturation-recovery signal of lipid spin labels in this membrane in the presence of oxygen. In the absence of oxygen, a single exponential fit is satisfactory. This fluid-fluid membrane microheterogeneity exists only up to 45°C and can be related to coexisting phases, the so-called liquid-ordered (l_o) and liquid-disordered (l_d) phases (Almeida et al., 1992). Two-component saturation-recovery signals of a fatty acid spin label were observed in the IFV membrane, indicating the presence of the SLOT domain (Kawasaki et al., 2001). However, saturation recovery signals exhibit more complex behaviour, and this case will be analyzed in detail below.

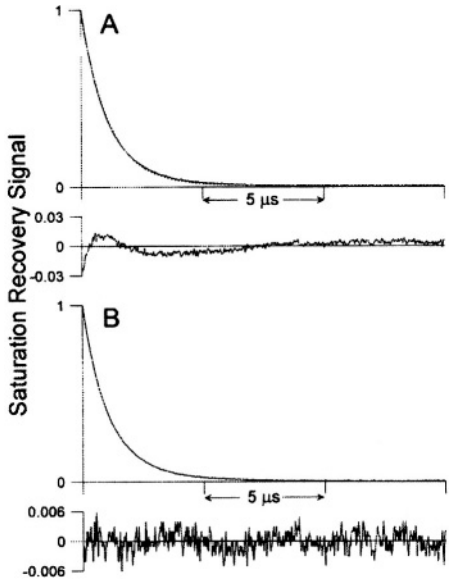

Figure 11. Saturation-recovery signal and curve fitting for 5-SASL in DMPC bilayer containing 20 mol% cholesterol. The recovery curve was obtained at 30°C for a sample equilibrated with 50% air in air/nitrogen mixture. Simulations and experimental saturation-recovery signals are superimposed for single-exponential fitting (A) and for double-exponential fitting (B). The difference between the experimental data and the fitted curve is shown in the lower part of each recovery curve. The time constants are 1.73 μs and 0.84 μs from the double-exponential fitting.

5.2 Exchange of Lipids Between the SLOT Domain and the BULK Domain (Outline of Theory)

In the following section, all equations will be expressed using electron spin transition rates; i.e.,

$$W_{10} = (1/2)T_1^{-1}(\mathrm{N_2}, \mathrm{SLOT}) \tag{18}$$

$$W_{20} = (1/2)T_1^{-1}(\mathrm{N_2}, \mathrm{BULK}) \tag{19}$$

$$W_1 = (1/2)T_1^{-1}(f_{\mathrm{air}}, \mathrm{SLOT}) \tag{20}$$

$$W_2 = (1/2)T_1^{-1}(f_{\mathrm{air}}, \mathrm{BULK}). \tag{21}$$

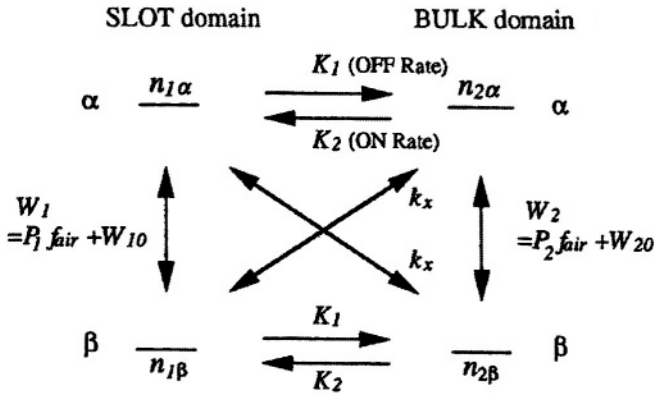

Figure 12. A scheme for analyzing saturation-recovery signals of spin labels in the presence of two domains that possess different oxygen transport rates: the SLOT domain and the BULK (bulk plus boundary) domain. An important point in this scheme is that it includes exchanges of lipid-type spin labels between the two domains (K_1 and K_2, outbound and inbound rates of the SLOT domain, respectively). The assumption is that all spin-label molecules are available for the exchange processes. In addition, this scheme includes the following two relaxation processes: (1) Electron spin transition of the spin label in each domain. The transition rates W_1 and W_2, are linear functions of the partial pressure of air, f_{air}, in the equilibrating gas mixture, W_{10} and W_{20} are the electron spin transition rates at $f_{air} = 0$, and $2P_1$ and $2P_2$ are the rates of oxygen collision with the spin label in a sample equilibrated with air. (2) Heisenberg exchange between the spins in different domains (k_X is the Heisenberg exchange rate). The three states of the doxyl nitrogen nuclear spin are assumed to mix into a single state because of fast nuclear spin relaxation (Popp and Hyde, 1982; see also Yin et al., 1987). The *n* values represent the instantaneous spin populations per unit volume of the four levels (from Kawasaki et al., 2001, © 2001, with permission from the Biophysical Society).

A theory has been developed to include the exchange of lipid-type spin labels between two domains that possess different oxygen transport rates (Kawasaki et al., 2001). The saturation-recovery signal of spin labels distributed between the two coexisting lipid domains in the membrane was analyzed based on the scheme shown in Fig. 12. Three relaxation processes are involved in saturation recoveries of spin labels exchanging between the two domains. The first is electron spin-lattice relaxation at each domain; the electron spin-lattice relaxation rates, W_1 and W_2, are linear functions of f_{air} ($W_1 = P_1 f_{air} + W_{10}$ and $W_2 = P_2 f_{air} + W_{20}$), and W_{10} and W_{20} are the electron spin-lattice relaxation rates at $f_{air} = 0$. The second process is the physical exchange of lipids (spin labels) between the two domains (K_1 and K_2 are the exchange rates). It is assumed that all spin label molecules are available for the exchange reaction, that is, the domains must be small for this formalism to be valid. The third is the Heisenberg exchange between the spins in different domains (k_x is the Heisenberg exchange rate).

Following Yin, Pasenkiewicz-Gierula and Hyde (1987), a set of rate equations was set up by Kawasaki et al. (2001) with the following solution:

$$I(t, f_{air}, N) = I_1[1 - \exp\{-(A - B)t\}] + I_2[1 - \exp\{-(A + B)t\}] \quad (22)$$

$$A(f_{air}, N) = W_1 + W_2 + (1/2)(K_1 + K_2 + k_X N) \quad (23)$$

$$B(f_{air}, N) = [(W_1 - W_2)^2 + (W_1 - W_2)\{K_1 - K_2 + (K_1 - K_2)k_X N/(K_1 + K_2)\} + (1/4)(K_1 + K_2 + k_X N)^2]^{1/2} \quad (24)$$

where $I(t, f_{air}, N)$ is the observed saturation-recovery signal, I_1 and I_2 are constants to be defined by initial conditions. The N represents the total number of spins per unit volume and is proportional to the number of spin probes incorporated in the membrane and the n values represent the instantaneous spin populations per unit volume of the four levels (see Fig. 12).

$$N = n_{1\alpha} + n_{1\beta} + n_{2\alpha} + n_{2\beta}. \quad (25)$$

As discussed below, all the rate constants (W_{10}, P_1, W_{20}, P_2, K_1, K_2, and k_X) are determined by obtaining saturation-recovery signals at various partial pressures of oxygen (at low spin-label concentrations), and at various concentrations of the spin label without oxygen. Dependencies of A and B^2 on oxygen concentration can be determined by the following equations obtained from Eqs. (20), (21), (23), and (24) (assuming $N = 0$, i.e., for a low concentration of the spin label):

$$\mathrm{A(fair) = (P_1 + P_2)fair + W_{10} + W_{20} + (1/2)(K_1 + K_2)} \quad (26)$$

$$B(f_{air})^2 = (P_1 - P_2)^2 f_{air}^2 + (P_1 - P_2)[2(W_{10} - W_{20}) + (K_1 - K_2)]f_{air} + (W_{10} - W_{20})^2 + (W_{10} - W_{20})(K_1 - K_2) + (1/4)(K_1 + K_2)^2 \quad (27)$$

Dependencies of A and $(A - B)(A + B)$ on the spin label concentration, N, in the absence of oxygen ($f_{air} = 0$) can be obtained from

$$A(N) = (1/2)k_X N + W_{10} + W_{20} + (1/2)(K_1 + K_2) \quad (28)$$

$$(A(N) - B(N))(A(N) + B(N)) = [W_{10} + W_{20}(W_{10} - W_{20})(K_1 - K_2)/(K_1 + K_2)]k_X N + 4W_{10}W_{20} + 2W_{10}K_2 + 2W_{20}K_1. \quad (29)$$

All coefficients on the right side of Eqs. (26-29) are determined by fitting the curves of A versus f_{air}, B^2 versus f_{air}, A versus N, and $(A - B)(A + B)$ versus N. Because there are only seven rate constants, all of them can be determined by solving these equations for coefficients.

5.3 Protein-Rich Rafts in Influenza Viral Membranes

The theory described above was applied to the analysis two-component saturation-recovery signals of a fatty acid spin label observed in the influenza viral (IFV) membrane (Kawasaki et al., 2001). The rate constants that were evaluated are listed in Table 2. The oxygen transport rate in the SLOT domain is smaller than in the BULK domain by a factor of 16. This suggests the possibility that the SLOT domain in the IFV membrane may not simply be a protein-rich region, but cholesterol rich and protein rich as well, because cholesterol can further reduce the oxygen collision rate (Subczynski et al., 1989, 1991a).

It has been proposed that the SLOT domain in the IFV membrane is the cholesterol-rich raft domain stabilized by the trimers of hemagglutinin and/or the tetramers of neuraminidase, the major protein components in the IFV membranes (Webster et al., 1982; Wilson et al., 1981; Varghese et al., 1983). The exchange rates from and to the SLOT domain were estimated to be 7.7 and 4.6×10^4 s^{-1}, respectively (Table 2). This indicates that the residency time of lipids in the SLOT domain is substantially longer than in the boundary region (East et al., 1985; Ryba et al., 1987; Horvath et al., 1988; Marsh, 1997), and suggests that the SLOT domain may play an important role in the function of the plasma membrane. Each individual SLOT domain may be small, but the entire SLOT domain occupies a substantial area within the IFV membrane. From the ratio of the inbound (K_2) to the outbound (K_1) rates of the lipid in the SLOT domain, the SLOT domains as a whole may occupy about one-third of the membrane.

5.4 Comments for Application of the DOT (Discrimination by Oxygen Transport) Method

It should be re-emphasized that the SLOT (slow oxygen transport) domain, which is a protein-rich raft domain in the IFV (influenza viral) membrane, is a dynamic structure. Either the constituent lipid molecules stay in the SLOT and BULK (bulk lipids plus boundary lipids) domains for less than 20 μs (the inverse of K_2, the slower exchange rate) or these domains are constantly formed and dispersed at an average of every 20 μs. The DOT method developed for analysis of pulse EPR spin label data using molecular oxygen as a probe is useful in studying SLOT domains,

particularly protein-stabilized cholesterol-rich raft domains, and the exchange of lipids between the SLOT domain and BULK domain. For more information see the recent review in this subject by Subczynski and Kusumi (2003).

Table 2: Evaluation of rate constants ($\times 10^6$ s^{-1}) described in Fig. 12 observed at 30°C in IFV membrane (from Kawasaki et al., 2001).

	SLOT domain	BULK domain
Oxygen transport parameter	$2P_1 = 0.14$	$2P_2 = 2.2$
Lipid exchange rate	$K_1 = 0.077$	$K_2 = 0.046$

6. OXIMETRY MEASUREMENTS CONFIRM QUALITY OF MOLECULAR DYNAMICS SIMULATION OF MEMBRANES

In the previous sections, we emphasized that molecular oxygen is a sensitive probe for studying membrane organization and dynamics, and noted that the oxygen transport parameter (Kusumi et al., 1982) is a sensitive and useful parameter to describe the three-dimensional dynamic structure of lipid bilayer membranes. Support for this statement also comes from molecular dynamics (MD) simulations. The idea of vacant pockets, which was introduced by Subczynski et al. (199la), is similar to the kink model presented by Trauble (1971) and Pace and Chan (1982). But the concept of vacant pockets covers a wider range of packing defects in the membrane and vacant pockets formed by a variety of mechanisms contribute to oxygen transport in the membrane. Oxygen molecules jump from one pocket to the adjacent one or move with the movement of the pocket itself due to rapid *gauche-trans* isomerization of phospholipid hydrocarbon chains. This hypothesis is supported by MD simulation, which shows that free voids exist in the hydrocarbon interior of the bilayer that are commonly large enough to accommodate small molecules such as oxygen or NO. These free voids are most common in the bilayer center (Stouch and Bassolino, 1996) which is reflected in profiles of the oxygen diffusion-concentration product (Kusumi et al., 1982; Subczynski et al., 1989, 1991a, 1998; Ashikawa et al., 1994).

MD simulations also indicate that small molecules (smaller than benzene) experience enhanced diffusion in the lipid bilayer membranes, with a diffusion rate a few times greater in the bilayer center (Stouch and Bassolino, 1996). This also agrees with oximetry measurements, which show that oxygen diffusion in membranes is as fast as in water, even though there may be a difference of one or two orders of magnitude in macroscopic viscosity (Subczynski and Hyde, 1981, 1984). Additionally, Kusumi et al. (1982) showed that oxygen diffusion in the fluid-phase PC bilayer is

isotropic, based on measurements of collision rates between oxygen and lipid-soluble spin labels with a different orientation of the π-orbital of the nitroxide radical relative to the membrane normal. This experimental result, which was criticized because the membrane is conventionally described as an anisotropic environment for the diffusion of small molecules, was confirmed by MD simulations of movement of other low molecular weight non-electrolytes in lipid bilayer membranes. For example, the calculated average coefficients of NO translational diffusion in both lateral and transversal directions in the phosphatidylcholine (PC) bilayer appear to be the same (Pasenkiewicz-Gierula and Subczynski, 1996). Similarly, the lateral diffusion coefficient profile of water molecules in a PC bilayer obtained from MD simulations was very similar to the transverse profile (Marrink and Berendsen, 1994).

The model based on MD simulations splits the lipid bilayer membrane into four regions, each of which has its own spatial characteristics. The exact location of the boundary regions are somewhat arbitrary; however, the qualitative idea of the four-region model is considered applicable to different bilayer membranes (Marrink and Berendsen, 1994). The first two regions belong to the head group region of the membrane (low and high density head group regions) while the other two regions describe the interior of the membrane (high and low tail density regions). On the basis of oxygen transport parameter measurements, three regions of the lipid bilayer membranes could be distinguished: the head group region with low oxygen transport and low activation energy of oxygen diffusion; the near head group region (the alkyl chain region up to the depth of about the ninth carbon) with a low oxygen transport parameter and higher activation energy of oxygen diffusion; and the central region where the oxygen transport parameter is a few times higher and activation energy is the lowest (Subczynski et al., 1989, 1991a, 1998). This discussion demonstrates that the spin-label oximetry approach is not only excellent for the study of membrane structure and dynamics, but also provides experimental information by which the quality of a membrane simulation can be assessed.

7. OXIMETRY *IN VIVO*

This topic has been reviewed comprehensively recently (Swartz and Clarkson (1998); Swartz (2003), and is discussed briefly in Ch. 9 by Swartz and Khan. Therefore we will cover only the general principles here and briefly describe some of the applications for both experimental and potential clinical uses. The measurement of pO_2 *in vivo* using EPR has some features that provide potential advantages for many applications. It already has led to

many very useful applications in animals and this clearly will expand significantly. There is a strong possibility that EPR oximetry also will have significant applications in clinical medicine.

The approaches and the applications differ depending on whether one uses soluble spin probes or particulates. The two approaches often are complimentary and sometimes can be used effectively in combination. The characteristics of EPR oximetry that appear to be especially useful often are complementary to existing techniques for measuring oxygen in tissues. These characteristics include capabilities of making repeated measurements from the same site (using particulates), imaging (using soluble probes), high sensitivity for low levels of oxygen, and non-invasive options. The existing EPR techniques are especially useful for studies in small animals, where the depth of measurements is not an over-riding issue. In larger animals and potentially in human subjects, the non-invasive techniques seem to be immediately applicable to study phenomena very near the surface (within 10 mm), while invasive techniques have some very promising uses for other sites. There also is a possibility of extending the non-invasive approach to greater depths by using lower frequency EPR. Measurements of pO_2 by EPR may take on added value when combined logically with other measurements that can be made especially well with *in vivo* EPR; for example it is possible to measure both nitric oxide and oxygen simultaneously (James et al., 1999a).

The clinical uses of EPR oximetry that seem especially promising and likely to be undertaken in the near future are based on the particulates. These include long term monitoring of the status and response to treatment of peripheral vascular disease and optimizing cancer therapy by enabling it to be modified on the basis of the pO_2 measured in the tumor. The *in vivo* applications of this technique have occurred because of the development of oxygen sensitive paramagnetic materials that are very sensitive to changes in the pO_2 and, in some cases, quite stable in tissues for long periods of time. These advances have been able to be used effectively because of instrumental developments that have made it feasible to make EPR measurements in intact animals.

Depending on the nature of the experiment and the techniques that are used, EPR oximetry can report on the $[O_2]$ or the pO_2 and can be used to study a wide range of oxygen levels from very low to well above physiological levels. Because of the versatility of EPR oximetry, usually a particular EPR oximetry technique will be optimal for a particular range of values or the types of measurements that are needed: e.g. whether single or repetitive, if repetitive for what length of time; the level of pO_2 that is likely to be encountered; whether data are needed as detailed maps (i.e. images), or

from paired sites, or from a single site; and the location of the site at which the measurement is to be made.

The volume that is resolved can vary from having a single volume which is defined by the size of the sample or the sensitive volume of the detector to having a full image composed of very small well-defined voxels. There are two extremes that often are termed spectroscopy and imaging respectively. There also are some alternatives between these two extremes, as noted below. The approach of choice usually will depend on the biological information that is being sought and the signal/noise that is available in the system.

The use of spectroscopy potentially has the advantage of maximum sensitivity. With spectroscopy all of the information is used for a single spectrum, potentially providing the best signal/noise achievable from the system. There also is the potential to obtain the maximum information content, with the full richness of the EPR spectrum being available. The disadvantage of spectroscopy is the limitation on spatial resolution of the information. With particulate paramagnetic materials (which can be as small as 100 microns), it is possible to obtain spectra from several sites simultaneously, when the particles are located in discrete positions and an appropriate magnetic field gradient is applied (Smirnov et al., 1993). In many situations this type of spatial resolution will be entirely sufficient for the purpose of the study.

Imaging techniques have the advantage of providing spatial resolution of the pO_2. Under some circumstances, especially when heterogeneity may be a large and important variable, this can be the biologically most important information. It is achieved, however, at the cost of the loss of signal/noise that is intrinsic with dividing the information into separate volumes and, potentially, the limitations on the information content in each resolved volume (usually this is limited to a single parameter such as intensity). Under conditions in which there is very good signal/noise, imaging can be combined with spectroscopy, providing spectral-spatial images in which much or all of the information content of the EPR spectrum is available in each voxel. In order to obtain a usable distribution of the oxygen-sensitive paramagnetic materials imaging, usually uses soluble paramagnetic materials; this leads to the need to readminister the compound for repeated measurements.

A potentially important approach for expanding the use of the oxygen sensitive paramagnetic materials is to encapsulate them in inert gas permeable materials such as plastics (Swartz and Walczak, 1996; Gallez et al., 1996; Gallez et al., 1998). This could have several advantages including extending the range and effectiveness of types of materials that can be used in experiments with animals and in accelerating the use of the oxygen

sensitive paramagnetic materials in human subjects. The use of appropriate materials would decrease or eliminate entirely the potential for undesired interactions between the paramagnetic materials and the tissues. This would facilitate the use of materials with excellent spectroscopic properties but whose responsiveness to oxygen is not sufficiently stable in some tissues (e.g. LiPc in skeletal muscle). It also is possible that some of the new materials will be found to have potentially toxic interactions with tissues and the coating would eliminate such interactions (e.g. some of the chars may cause effects by binding biologically important materials to their surfaces, potentially depleting them locally). The feasibility of the use of encapsulation has been demonstrated *in vitro* and in limited experiments in animals, and there do not appear to be any substantial obstacles to this approach. The use of encapsulation could be combined with some of the more invasive approaches that have been suggested to extend the depth at which measurements can be made at the higher range of frequencies, such as the catheter-needle probe and the implantable resonator. For the latter the paramagnetic material could be positioned at a site within the resonator where there would be maximum sensitivity. Encapsulation also would make it feasible immediately to use other materials in addition to India ink in human subjects. These could be in the form of macroscopic structures which then could be removed when the observation period was completed and thereby avoid the potential problems involved with the evaluation of the effects of materials which are permanently present in tissues. If the encapsulating materials are substances that are approved for permanent placement in tissues, then it would not be necessary to remove them even at the end of the observation period.

A number of studies have demonstrated that when inserted properly and allowed to reach equilibration, the paramagnetic materials do not perturb the local pO_2 as measured by other techniques and physiological parameters. It is necessary, of course, to ensure in each experimental setup that the presence of the paramagnetic material has not unduly disturbed the physiology. The physiological/pathophysiological meaning of these measurements depends on the particular study but when appropriate considerations are used, the data can provide very useful information.

The soluble paramagnetic materials can have lifetimes for oximetry that range from seconds to hours. The principal factors affecting these lifetimes are the extent of metabolism to non-paramagnetic forms and excretion. The particulate materials usually have much longer biological lifetimes, but their responsiveness to oxygen may not persist even though they remain in situ without obvious reactions of the tissues to their presence. The long term stability of the responsiveness to oxygen that can be achieved with the particulate paramagnetic materials under certain conditions varies from

relatively short term for LiPc in muscle (about a week) to very long term (probably years or more) for most of the carbon-based materials and LiPc in some environments (e.g. the spinal cord).

Both imaging and spectroscopy of pO_2 have been achieved with the soluble paramagnetic materials. While most of the results to date with the particulate materials have used spectroscopy with localization defined by the position of the particles, with the use of a magnetic field gradient the method has been able to resolve spectra at multiple sites simultaneously. Useful results with multisite spectroscopy have been obtained in the heart (Smirnov et al., 1993), kidneys (James et al., 1996), brain (Liu et al., 1995), and tumors (Grinberg et al., 2001).

The study of fast processes has been accomplished principally with spectroscopy with particulate materials, although very impressive time-resolved studies in the heart have been obtained by gated acquisition of images of soluble nitroxides in the isolated heart (see chapter 16). With spectroscopy of particles, time resolution of the order of seconds to minutes has been achieved. In the heart, for example, the first point at 15 seconds showed the full response (Swartz et al., 1994) and less than a minute was resolved in kidney, skeletal muscle, and brain (Liu et al., 1993).

7.1 Measurements in Tumors

The most extensive applications of EPR oximetry are likely to be in tumors because of the close relationship between the pO_2 and tumor therapy. The response of tumors to ionizing radiation and, in some cases, to chemotherapy, is greatly affected by the local amount of oxygen, with the sensitivity decreasing by up to a factor of three when the partial pressure is below 5-10 torr. EPR oximetry has the potential to make such measurements accurately and, perhaps most importantly, on a repeated basis.

So far, most of the studies have been done at 1200 MHz but, using a very low frequency *in vivo* EPR spectrometer (250 ± 20 MHz) Halpern et al (1994; 1996) measured the concentration of oxygen in a fibrosarcoma in mice and the effect of perfluorocarbon/carbogen on the oxygen concentration, using a specially designed nitroxide which also has the potential for providing information on viscosity.

The potential value of *in vivo* EPR for following the pO_2 in tumors has been shown with the particulate oxygen sensitive paramagnetic materials (Swartz et al., 1994; Goda et al., 1995a, 1995b; O'Hara et al., 1995, 1997b, 1998; James et al., 199b; Pogue et al., 1999). After placing one or more deposits of oxygen sensitive paramagnetic materials at sites of interest in rodents and then making repeated measurements over several days or weeks using restrained but awake animals and a surface detector it has been shown

to be feasible to: measure the pO_2 in several different types of tumors; follow changes in pO_2 during growth; measure the effects of therapy on the pO_2 in tumors; use radiation-induced changes in pO_2 to enhance the effectiveness of subsequent doses of radiation by delivering these doses at the time when the pO_2 was relatively high; and combine EPR oximetry with NMR techniques (Dunn et al., 1995). These approaches have the potential of providing clinical physicians with a method to individualize therapy for each patient by selecting the appropriate type and timing of treatment on the basis of the pO_2 measured in the patient's tumor both initially and then during the course of therapy (O'Hara et al., 1997a, 1998).

While technically more challenging, EPR imaging of tumors has considerable potential for both basic and applied studies in which the distribution of oxygen can be defined and followed. It has been an important motivation for the development of imaging (Sotgiu, 1985; Nishikawa et al., 1985; Halpern et al., 1986, 1989). There have been several studies in model systems that have demonstrated the potential of EPR imaging to measure and image oxygen concentrations in living systems. Halpern et al. (1994) have published an oxygen sensitive 2-D (one spatial dimension) full spectral-spatial image of a mouse tumor. In this proof of principle study, the oxygen tension resolution was approximately 5 torr and the spatial resolution was 5 mm. This initial tumor image shows lower oxygen tension in the center of the tumor mass than in the periphery, consistent with the expectation of an hypoxic tumor core. See ch. 11 by Williams and Halpern for more recent results showing improved resolution.

7.2 Brain and Spinal Cord

EPR oximetry provides a potentially very useful method directly to follow changes in the pO_2 under various physiological and pathophysiological conditions in this organ whose metabolism usually involves a high rate of oxidative phosphorylation, and therefore the brain potentially is quite vulnerable to changes in the pO_2. This seems especially useful for situations in which repeated measurements of brain pO_2 are needed over a period of time. LiPc has been especially useful for *in vivo* studies of the pO_2 in the central nervous system because of its sensitivity to the relatively high concentrations of oxygen that occur normally in these tissues. Some results already have been obtained with *in vivo* EPR on the pO_2 in brain as a function of the breathing gas, with the use of various anesthetics, on adaptations to chronic hypoxia of the type likely to occur at high altitudes, and to monitor the extent of ischemia and reperfusion (Liu et al., 1993, 1995, 1997; Taie et al., 1999; Grinberg et al., 2000). These studies included the use of more than one site at which the pO_2 was measured

simultaneously, providing a very effective comparison between the experimentally manipulated side and the control side in the brain. EPR oximetry also has been used effectively to follow the effects of ionizing radiation on the pO_2 in the spinal cord, demonstrating an unexpected increase of pO_2 in animals followed for up to 9 months.

7.3 Heart

Oxygen has a critically important role in this organ because of the high rate of aerobic metabolism but direct studies have been difficult because of the motion. EPR oximetry provides a means to make such measurements in a non-destructive manner with the accuracy and sensitivity needed for these measurements. While a few oximetry studies have been carried out in the heart in situ in the rat, most of the EPR oximetry studies of the heart have used the isolated beating heart. These studies have provided some excellent insights into various physiological parameters that affect the level of oxygen in the wall of the heart, the effects of some drugs on the pO_2 in the heart, and the effects of treatments such as "ischemic preconditioning" (Friedman et al., 1995, 1996; Grinberg et al., 1997a, 1997b). As EPR oximetry has developed it has been increasingly used in combination with other measures of cardiac function. This enables the information provided by EPR oximetry to be used most effectively to unravel pathophysiology. Using this approach it has been possible to investigate the hypothesis that cardiomyopathy can be a result of an autoimmune process in which the distribution of oxygen becomes quite heterogeneous (Friedman et al., 1998). In this case the crucial experimental result was an increase in the scatter of the values for myocardial pO_2 rather than a change in absolute pO_2. The relationship of the amount of oxygen in the heart to oxidative damage associated with ischemia-reperfusion injury is another critical issue which has been able to be investigated using EPR oximetry in combination with the unique capabilities of EPR also to measure directly free radicals (Kuppusamy et al., 1994; Zweier et al., 1991).

7.4 Skeletal Muscle

The measurement of pO_2 in skeletal muscle is of great interest for understanding the energetics of muscle function. It would be especially valuable to be able to relate the pO_2 to measurements of key metabolites such as those that can be measured by NMR (e.g. ATP, inorganic phosphate, and lactic acid). EPR oximetry appears to have the capability for making the desired measurement of pO_2 in skeletal muscle and some results have been reported using both carbon-based materials and LiPc (Chan et al., 1989;

Glockner et al., 1991; Glockner and Swartz 1992) and also nitroxides in cyclohexane filled albumin microspheres (Liu et al., 1994).

7.5 Liver

The liver has a very complex blood supply, receiving blood via both the hepatic artery and the portal vein. It also has a complex microscopic anatomy in regard to the circulation of blood, with input from the portal triad, distribution via the sinusoids, and then collection via the central veins. As a consequence the liver has a number of pathophysiological conditions which seem to be very much affected by the local pO_2, but conventional methods are difficult to use in this organ. Consequently, EPR oximetry has been used to study pO_2 in the liver and some useful and interesting data already have emerged (Glockner et al., 1991; Goda et al., 1995a; Nakashima et al., 1995a, 1995b; Jiang et al., 1996). It is possible to use the different physical properties of the paramagnetic materials and/or the way that they are administered to affect their localization within the liver and thereby obtain measurements at functionally different sites within the liver. The use of either liposomes of the appropriate size or particles of India ink results in the selective accumulation of the paramagnetic material in the Kupffer cells and therefore provides measurements of the pO_2 at this site. Average global pO_2 can be obtained with the use of macroscopic materials such as crystals of lithium phthalocyanine. Using both types of measurements in the same animal, some preliminary evidence was obtained which indicates that the pO_2 in the Kupffer cells may be lower than in hepatocytes. The effects of acute ligation on the pO_2 also were studied. The effects on the pO_2 in the Kupffer cells from the hepatotoxin, carbon tetrachloride, were able to be followed over a two-week period, using India ink particles that had localized in the Kupffer cells (Nakashima et al., 1995a).

7.6 Kidney

The number of measurements of levels of oxygen in the kidney are limited because of the technical difficulties of making such measurements. The difficulties arise because of the deep location of the kidneys, the complex pattern of blood supply within the kidney, and the motion of the kidneys due to respiration. Therefore, the capabilities of EPR oximetry may be very important and useful for this organ. Some results already have been reported for EPR measurements of the pO_2 in both isolated perfused kidneys and *in vivo* (Liu et al., 1993; James et al., 1996, 1997, 1999b). The techniques used for these measurements included simultaneous measurements in the cortex and medulla of the kidney; these are useful

because of their different blood supplies and different responses to changes in the circulatory system. As expected from results with other techniques, the baseline pO_2 of the cortex was higher than that of the medulla. In response to the injection of endotoxin the pO_2 of the medulla increased while that of the cortex decreased, and the two became approximately equal. This effect could be eliminated by the administration of an inhibitor of nitric oxide synthase, suggesting that the effect was mediated by nitric oxide. It also is possible to use *in vivo* EPR to measure the nitric oxide directly (James et al., 1999b).

7.7 Skin and Underlying Tissues

Within the skin there are a number of processes that should be greatly affected by the amount of oxygen, including burns and wounds, especially in regard to factors that may affect the rate of healing. If one extends the definition of skin to include the immediately underlying tissues including some muscles, then this encompasses a region of great potential clinical utility: the status of the tissues at risk in peripheral vascular disease (Swartz and Walczak 1996, 1998). Because of its location, the skin is fully accessible to the relatively higher frequency *in vivo* EPR (e.g. 1200 MHz), in contrast to many other sites where depth of sensitivity can be limiting. To date there are only a few reported studies of EPR oximetry in skin (Hatcher et al., 1993; Swartz et al., 1994; Goda et al., 1995a), but it seems likely that this will change in the near future. The areas that are likely to have particular emphasis include wound healing and peripheral vascular disease. There is a considerable potential for early clinical studies using EPR oximetry in skin, including the potential of taking advantage of the properties of India ink for EPR oximetry.

8. FINAL REMARKS

Spin-label oximetry permits measurement of the collision rate of molecular oxygen with the nitroxide moiety of spin labels, and calculation of the product of the local oxygen diffusion coefficient and the local oxygen concentration. Separation of this product into component factors, diffusion and concentration, is, however, inherently difficult. Bimolecular collision occurs at the molecular level, while the concentration and diffusion are bulk properties of the surrounding medium. In homogenous fluids, such as the aqueous phase, separation is possible and has been verified. In a heterogeneous system, separation seems intrinsically impossible. Good examples of heterogeneous systems for which spin-label oximetry is

intensively applied are macromolecules with specifically attached spin labels, or anisotropic lipid bilayer membranes with spin labels placed at a certain depth. For the latter system, an average oxygen concentration in the lipid bilayer was obtained in conceptually different experiments (Subczynski and Hyde, 1983; Smotkin et al., 1991).

ACKNOWLEDGMENTS

This work was supported by grants RR01008, GM27665 and GM61236 from the National Institute of Health of the U.S.A. (WKS) and the NCRR supported EPR Center for Viable Systems, NIH grant P41RR11602 and NCI grant P01CA91597.

9. REFERENCES

Ahn, M.-K. (1976) Diffusion coefficients of paramagnetic species in solution, *J. Magn. Reson.* **22**, 289-293.

Almeida, P. F. F., Vaz, W. L. C., and Thompson, T. E. (1992) Lateral diffusion in the liquid phase of dimyristoylphosphatidylcholine/cholesterol bilayers: A free volume analysis, *Biochemistry* **31**, 6739-8747.

Altenbach, C., Greenhalgh, D. A., Khorana, H. G., and Hubbell, W. L. (1994) A collision gradient method to determine the immersion depth of nitroxides in lipid bilayers: Application to spin-labeled mutants of bacteriorhodopsin, *Proc. Natl. Acad. Sci. USA* **91**, 1667- 1671.

Altenbach, C., Marti, T., Khorana, H. G., and Hubbell, W. L. (1990) Transmembrane protein structure: Spin labeling of bacteriorhodopsin mutants, *Science* **248**, 1088-1092.

Ardenkjaer-Larsen, J. H., Laursen, I., Leunbach, I., Ehnholm, G., Wistrand, L.-G., Petersson, J. S., and Golman, K. (1998) EPR and DNP properties of certain novel single electron contrast agents intended for oximetric imaging, *J. Magn. Reson.* **133**, 1-12.

Ankel, E., Felix, C. C., and Kalyanaraman, B. (1986) The use of spin label oximetry in the study of photodynamic inactivation of Chinese hamster ovary cells, *Photochem. Photobiol.* **44**, 741-746.

Ashikawa, L, Yin, J.-J., Subczynski, W. K., Kouyama, T., Hyde, J. S., and Kusumi, A. (1994) Molecular organization and dynamics in bacteriorhodopsin-rich reconstituted membranes: discrimination of lipid environments by the oxygen transport parameter using a pulse ESR spin-labeling technique, *Biochemistry* **33**, 4947-4952.

Backer, J. M., Budker, V. G., Eremenko, S. I., and Molin, Yu. N. (1977) Determination of the kinetics of biochemical reactions with oxygen using exchange broadening in the ESR spectra of nitroxide radicals, *Biochim. Biophys. Acta* **460**, 152-156.

Bielec, J., Pilas, B., Sarna, T., and Truscott, T. G. (1986) Photochemical studies of phorphyrin-melanin interactions, *J. Chem. Soc. Faraday Trans.* **282**, 1469-1474.

Boag, J. W. (1969) Oxygen diffusion and oxygen depletion problems in radiobiology, *Curr. Top. Radiobiol. Res.* **5**, 141-195.

Chan, H.-C., Glockner, J. F., and Swartz, H. M. (1989) Oximetry in cells and tissue using a nitroxide-liposome system, *Biochim. Biophys. Acta* **1014**, 141-144.

Diamond, J., and Katz, Y. (1970) Interpretation of nonelectrolyte partition coefficients between dimyristoyl lecithin and water, *J. Membr. Biol.* **17**, 121-154.

Dunn, J. F., Ding, S., O'Hara, J. A., Liu, K. J., Rhodes, E., Weaver, J. B., and Swartz, H. M. (1995) The apparent diffusion constant measured by MRI correlates with pO_2 in a RIF-1 tumor, *Magn. Reson. Med.* **34**, 515-519.

East, J. M., Melville D., and Lee, A. G. (1985) Exchange rates and numbers of annular lipids for the calcium and magnesium ion dependent adenosine triphosphate, *Biochemistry* **24**, 2615-2623.

Farahbakhsh, Z. T., Altenbach, C., and Hubbell, W. L. (1992) Spin labeled cysteins as sensors for protein-lipid interaction and conformation in rhodopsin, *Photochem. Photobiol.* **56**, 1019-1033.

Feix, J. B., and Klug, C. S. (1998) Site-directed spin labeling of membrane proteins and peptide-membrane interaction, in *Biological Magnetic Resonance, Vol. 14. Spin Labeling: The Next Millennium,* L. J. Berliner, Ed., Plenum Press, New York, 251-281.

Friedman, B. J., Grinberg, O. Y., Isaacs, K.., Walczak, T. M., and Swartz, H. M. (1995) Myocardial oxygen tension and relative capillary density in isolated perfused rat hearts. *J. Mol. Cell Cardiol.* **27**, 2551-2558.

Friedman, B. J., Grinberg, O. Y., Isaacs, K., Ruuge, E. K., and Swartz, H. M. (1996) Effect of repetitive ischemia on local myocardial oxygen tension in isolated perfused and hypoperfused rat hearts, *Magn. Reson. Med.* **35**, 214-220.

Friedman, B. J., Grinberg, O. Y., Ratcliffe, N. R., Swartz, H. M., and Hickey, W. F. (1998) Acute hemodynamic and coronary circulatory of experimental autoimmune myocarditis, *Heart Vessels* **13**, 58-62.

Froncisz, W., and Hyde, J. S. (1982) The loop-gap resonator: A new microwave lumped circuit ESR sample structure, J. *Magn. Reson.* **47**, 515-521.

Froncisz, W., Lai, C.-S., and Hyde, J. S. (1985) Spin-label oximetry: Kinetic study of cell respiration using a rapid-passage T_1-sensitive electron spin resonance display, *Proc. Natl. Acad. Sci. USA* **82**, 411-415.

Gaidarov, I., Santini, F., Warren, R. A., and Keen, J. H. (1998) Spatial control of coated-pit dynamics in living cells, *Nat. Cell Biol.* **1**, 1-7.

Gallez, B., Debuyst, R., Liu, K. J., Demeure, R., Dejehet, F., and Swartz, H. M. (1996) Development of biocompatible implants of fusinite for *In Vivo* oximetry, *MAGMA* **4**, 71-75.

Gallez, B., Debuyst, R., Dejehet, F., Liu, K. J., Walczak, T., Swartz, H. M., Goda, F., Demeure, R., and Taper, H. (1998) Small particles of fusinite and carbohydrate chars coated with aqueous soluble polymers: preparation and applications for *In Vivo* EPR oximetry. *Magn. Reson. Med.* **40**, 152-159.

Glockner, J. F., Chan, H.-C., and Swartz, H. M. (1991) *In Vivo* oximetry using a nitroxide-liposome system, *Magn. Reson. Med.* **20**, 123-133.

Glockner, J. F., Norby, S.-W., and Swartz, H. M. (1993) Simultaneous measurement of intracellular and extracellular oxygen concentration using a nitroxide-liposome system, *Magn. Reson. Med.* **29**, 12-18.

Glockner, J. F., and Swartz, H. M. (1992) *In Vivo* EPR oximetry using two novel probes: fusinite and lithium phthalocyanine, in *Adv. Exp. Biol. Med.,* **317**, W. Erdmann and D. F. Bruley, Eds., Plenum Press, New York, 229-234.

Glockner, J. F., Swartz, H. M., and Pals, M. A. (1989) Oxygen gradients in CHO cells: Measurement and characterization by electron spin resonance, *J. Cell Physiol.* **140**, 505-511.

Goda, F., Liu, K. J., Walczak, T., O'Hara, J. A., Jiang, J., and Swartz, H. M. (1995a) *In vivo* oximetry using EPR and Indian ink, *Magn. Reson. Med.* **33**, 237-245.

Goda, F., O'Hara, J. A., Rhodes, E. S., Liu, K. J., Dunn, J. F., Bacic, G., and Swartz, H. M. (1995b) The changes of oxygen tension in experimental tumors after a single dose of X-ray irradiation, *Canc. Res.* **55**. 2249-2252.

Grinberg, O. Y., Friedman, B. J., and Swartz, H. M. (1997a) Intramyocardial pO_2 measured by EPR, *Adv. Exp. Med. Biol.* **428**, 261-268.

Grinberg, O. Y., Grinberg, S. A., Friedman, B. J., and Swartz, H. M. (1997b) Myocardial oxygen tension and capillary density in the isolated perfused rat heart during pharmacological intervention, *Adv. Exp. Med. Biol.* **411**, 171-181.

Grinberg, O. Y., Hou, H., and Swartz, H. M. (2000) Direct repeated measurements of pO_2 in the brain during ischemia and reperfusion, *Ischemic Blood Flow in the Brain* (Y. Fukuuchi, M. Tomita and A. Koto, eds.), **6**:381-389. Springer-Verlag Tokyo. Keio University Symposia for Life Science and Medicine.

Grinberg, O. Y., Smirnov, A.I., and Swartz, H.M. (2001) High spatial resolution multi-site EPR oximetry: the use of a convolution-based fitting method, *J. Magn. Reson.* **152**, 247-258.

Halpern, H. J., Bowman, M. K., Spencer, D. P., van Polen, J., Dowey, E. M., Massoth, R. J., Nelson, A. C., and Teicher, B. A. (1989) An imaging radiofrequency electron spin resonance spectrometer with high resolution and sensitivity for in vivo measurements, *Rev. Sci. Instr.* **60**, 1040-1050.

Halpern, H. J., Chandramouli, G. V. R., Williams, B. B., Barth, E. D., and Galtsev, V. (1998) Challenge of 3- and 4-dimensional *in vivo* spectral spatial EPR imaging at radiofrequency with narrow line spin resonance, *Twenty first International EPR Symposium,* Denver, Abstract No. 124.

Halpern, H. J., Perik, M., Nguyen, T-D., Spencer, D. P., Teicher, B. A., and Lin, Y. J. (1990) Selective isotopic labeling of a nitroxide spin label to enhance sensitivity for T2 oximetry, *J. Magn. Reson.* **90**, 40-51.

Halpern, H. J., Spencer, D. P., van Polen, J., Bowman, M. K., Massoth, R. J., Teicher, B. A., Downy, E. M., and Nelson, A. C. (1986) A low frequency imaging electron spin resonance spectrometer for non-invasive measurement of tumor oxygenation and other parameters characterizing tumor radiosensitivity, *Radiation Oncology/Biology/Physics* **12**, 217-218.

Halpern, H. J., Yu, C., Peric, M., Barth, E., Grdina, D. J., and Teicher, B. A. (1994) Oxymetry deep in tissues with low-frequency electron paramagnetic resonance, *Proc. Natl. Acad. Sci. USA* **91**, 13047-13051.

Hatcher, M. E., and Plachy, W. Z. (1993) Dioxygen diffusion in the stratum corneum: An EPR spin label study. *Biochim. Biophys. Acta.*. **1149**, 73-78.

Hitchman, M. L., 1978, *Measurement of Dissolved Oxygen.* Wiley, NY.

Holland, R. A. (1967) Kinetics of combination of O_2 and CO with human hemoglobin F in cells and in solution, *Respir. Physiol.* **3**, 307-317.

Horváth L. I., Brophy, P. J., and Marsh, D. (1988) Exchange rates at the lipid-peptide interface of myelin proteolipid protein studied by spin-label electron spin resonance, *Biochemistry* 27, 46-52.

Hu, H., Sosnovsky, G., and Swartz, H. M. (1992) Simultanous measurements of the intra- and extra-cellular oxygen concentration in viable cells, *Biochim. Biophys. Acta* **1112**, 161-166.

Hyde, J. S., and Subczynski, W. K. (1984) Simulation of ESR spectra of the oxygen-sensitive spin-label probe CTPO, *J. Magn. Reson.* **56**, 125-130.

Hyde, J. S., and Subczynski, W. K. (1989) Spin-label oximetry, in *Biological Magnetic Resonance. Vol. 8. Spin Labeling. Theory and Applications,* L. J. Berliner and J. Reuben, Eds. Plenum, New York, 399-425.

Hyde, J. S., Subczynski, W. K., Froncisz, W., and Lai, C.-S. (1983) Spin label oximetry: Measurement of oxygen concentration in biological samples, *Bull. Magn. Reson.* **5,** 180-182.

Ito, J. S., Uede, M. J., Okuda, T. S., and Ohnishi, S. I. (1981) Phagocytosis by macrophages II. The dissociation of the attachment and ingestion steps, *J. Cell Sci.* **51,** 189-201.

James, P. E., Bacic, G., Grinberg, O. Y., Goda, F., Dunn, J., Jackson, S. K., and Swartz, H. M. (1996) Endotoxin induced changes in intrarenal pO_2 measured by *in vivo* electron paramagnetic resonance oximetry and magnetic resonance imaging, *Free Rad. Biol. Med.* **21,** 25-34.

James, P.E., Grinberg, O. Y., Goda, F., Panz, T., O'Hara, J. A., and Swartz, H. M. (1997) Gloxy: an oxygen-sensitive coal for accurate measurement of low oxygen tensions in biological systems, *Magn. Reson. Med.* **37,** 48-58.

James, P. E., Miyake, M., and Swartz, H. M. (1999a) Simultaneous measurement of NO and pO_2 from tissue by *in vivo* EPR, *Nitric Oxide: Biology and Chemistry* **3,** 92-301.

James, P. E., O'Hara, J. A., Grinberg, S. A., Panz, T., and Swartz, H. M. (1999b) Impact of the antimetastatic drug batimastat on tumor growth and pO_2 measured by EPR oximetry in a murine mammary adenocarcinoma, *Adv. Exp. Med. Biol.* **471,** 487-496.

Jiang, J., Nakashima, T., Shima, T., Liu, K. J., Goda, F., and Swartz, H. M. (1996) Measurement of pO_2 in liver using EPR oximetry, *J. of Appl. Physiol.* **80,** 552-558.

Kalyanaraman, B., Feix, J. B., Sieber, F., Thomas, J. P., and Girotti, A. W. (1987) Photodynamic action of merocyanine 540 on artificial and natural cell membranes: Involvement of singlet molecular oxygen, *Proc. Natl. Acad. Sci. USA* **84,** 2999-3003.

Kawasaki, K., Yin, J.-J., Subczynski, W. K., Hyde, J. S., and Kusumi, A. (2001) Pulse EPR detection of Hpid exchange between protein-rich raft and bulk domains in the membrane: Methodology development and its application to studies of influenza viral membrane, *Biophys. J.* **80,** 738-748.

Kuppusamy, P., Chzhan, M., Vij, K., Shteynbuk, M., Lefer, D. J., Giannella, E., and Zweier, J. L. (1994) Three-dimensional spectral-spatial EPR imaging of free radicals in the heart: a technique for in vivo imaging of tissue metabolism and oxygenation, *Proc. Natl. Acad. Sci.* USA **91,** 3388-3392.

Kusumi, A., Subczynski, W. K., and Hyde, J. S. (1982) Oxygen transport parameter in membranes as deduced by saturation recovery measurements of spin-lattice relaxation times of spin labels, *Proc. Natl. Acad. Sci. USA* **79,** 1854-1858.

Lai, C.-S., Hopwood, L. E., Hyde, J. S., and Lukiewicz, S. J. (1982) ESR studies of O_2 uptake by Chinese hamster ovary cells during the cell cycle, *Proc. Natl. Acad. Sci. USA* **79,** 1854-1858.

Ligeza, A., Swartz, H. M., and Subczynski, W. K. (1994) Spin-label oximetry in dense cell suspensions: Problems in closed- and open-chamber methods, *Curr. Top. Biophys.* **18,** 29-38.

Ligeza, A., Tikhonov, A. N., and Subczynski, W. K. (1997) *In situ* measurements of oxygen production and consumption using paramagnetic fusinite particles injected into a bean leaf, *Biochim. Biophys. Acta* **1319,** 133-137.

Ligeza, A., Tikhonov, A., Hyde, J. S., and Subczynski, W. K. (1998) Oxygen permeability of thylakoid membranes: Electron paramagnetic resonance spin labeling study, *Biochim. Biophys. Acta* **1365,** 453-463.

Ligeza, A., Wisniewska, A., and Subczynski, W. K. (1992) Paraffin oil particles as microscopic probes for oxygen measurement in biological systems: ESR spin-label oximetry, *Curr. Top. Biophys.* **16,** 92-98.

Linke, W. F. (1965) *Solubilities: Inorganic and metal organic compounds* II. 4th ed. American Chemical Society, Washington, DC, 1233-1236.

Liu, K. J., Bacic, G., Hoopes, P. J., Jiang, J., Dunn, J. F., and Swartz, H. M. (1995) Assessment of cerebral pO_2 by EPR oximetry in rodents: effects of anesthesia, ischemia, and breathing gas, *Brain Res.* **685,** 91-98.

Liu, K. J., Gast, P., Moussavi, M., Norby, S. W., Vahidi, N., Walczak, T., Wu, M., and Swartz, H. M. (1993) Lithium phtalocyanine: A probe for electron paramagnetic resonance oximetry in viable biological systems, *Proc. Natl. Acad. Sci. USA* **90,** 5438-5442.

Liu, K. J., Grinstaff, M. W., Jiang, J. J., Suslick, K. S., Swartz, H. M., and Wang, W. (1994) *In vivo* measurement of oxygen concentration using sonochemically synthesized microspheres, *Biophys. J.* **67,** 896-901.

Liu, K. J., Hoopes, P. J., Rolett, E. L., Beerle, B., Azzawi, A., Goda, F., Dunn, J. J., and Swartz, H. M. (1997) Effect of anesthesia on cerebral tissue oxygen and cardiopulmonary parameters in rats, *Adv. Exp. Med. Biol.* **428,** 33-39.

Liu, X., Miller, M. J. S., Joshi, M. S., Thomas, D. D., and Lancaster, J. R. (1998) Accelerated reaction of nitric oxide with O_2 within the hydrophobic interior of biological membranes, *Proc. Natl. Acad. Sci. USA* **95**, 2175-2179.

Lomnicka, M., and Subczynski, W. K. (1996) Spin-label NO-metry, *Curr. Top. Biophys.* **20,** 76-80.

Lukiewicz, S. J. (1985) *In vivo* electron spin resonance spectroscopy, *Radio and Microwave Spectr.* **54,** 37-54.

Lukiewicz, S. J., and Lukiewicz, S. G. (1984) *In vivo* ESR spectroscopy of large biological objects, *Magn. Reson. Med.* **1,** 297-298.

Marrink, S.-J., and Berendsen, H. J. C. (1994) Simulation of water transport through a lipid membrane, *J. Phys. Chem.* **98,** 4155-4168.

Marsh, D. (1997) Stoichiometry of lipid-protein interaction and integral membrane protein structure, *Eur. Biophys. J.* **26,** 203-208.

Marsh, D. (2001) Polarity and permeation profiles in lipid membranes, *Proc. Natl. Acad. Sci. USA* **98,** 7777-7782.

Marsh, D., and Watts, A. (1981) ESR spin label studies of liposomes, in *Liposomes: from Physical Structure to Therapeutic Applications,* C. G. Knight, Ed., Elsevier/North-Holland Biomedical Press, Amsterdam, 139-188.

Mchaourab, H. S., and Hyde, J. S. (1993) Dependence of the multi-quantum EPR signal on the spin lattice relaxation time. Effect of oxygen in spin-labeled membranes, *J. Magn. Reson. B* **101,** 178-184.

Mchaourab, H. S., Hyde, J. S., and Feix, J. B. (1994) Binding and state of aggregation of spin-labeled ceocropin AD in phospholipid bilayer: Effects of surface charge and fatty acyl chain length, *Biochemistry* **33,** 6691-6699.

McIntosh, T. J. (1978) The effect of cholesterol on the structure of phosphatidylcholine bilayers, *Biochim. Biophys. Acta* **513,** 43-58.

Miettinen, H. M., Matter, K., Hunziker, W., Rose., J. K., and Mellman, I. (1992) Fc receptor endocytosis is controlled by cytoplasmic domain determinant that actively prevents coated pit localization, *J. Cell Biol.* **116,** 875-888.

Molin, Y. N., Salikhov, K. M., and Zamaraev, K. I. (1980) *Spin Exchange,* Springer-Verlag, New York, 111-115.

Morrow, M. R., Huschilt, J. C., and Davis, J. H. (1985) Simultaneous modeling of phase and calorimetric behavior in an amphiphilic peptide/phospholipid model membrane, *Biochemistry* **24,** 5396-5406.

Morse II, P. D., and Swartz, H. M. (1985) Measurement of intracellular oxygen concentration using the spin label TEMPOL, *Magn. Reson. Med.* **2,** 114-127.

Nakashima, T., Jiang, J,, Goda, F., Shima, T., and Swartz, H. M. (1995a) The measurement of pO_2 in mouse liver *in vivo* by EPR oximetry using India ink, *Magn. Reson. Med. (Japan)* **6,** 158-160.

Nakashima, T., Goda, F., Jiang, J., Shima, T., and Swartz, H. M. (1995b) Use of EPR oximetry with India ink to measure the pO_2 in the liver *in vivo* in mice, *Magn. Reson. Med.* **34,** 888-892.

Nicholson, P., and Roughton, F. J. W. (1951) A theoretical study of the influence of diffusion and chemical reaction velocity on the rate of exchange of carbon monoxide and oxygen between the red blood corpuscle and surrounding fluid, *Proc. Roy. Soc. B* **138,** 241-264.

Nishikawa, H., Fujii, H., and Berliner, L. J. (1985) Helices and surface coils for low-field *in vivo* ESR and EPR imaging applications, *J. Magn. Reson.* **62,** 79-86.

O'Hara, J. A., Goda, F., Demidenko, E., and Swartz, H. M. (1998) Effect on regrowth delay in a murine tumor of scheduling split dose irradiation based on direct pO_2 measurements by electron paramagnetic resonance oximetry, *Radiat. Res.* **150,** 549-556.

O'Hara, J. A., Goda, F., Dunn, J. F., and Swartz, H. M. (1997a) Potential for EPR oximetry to guide treatment planning for tumors, *Adv. Exp. Med. Biol.* **428,** 233-242.

O'Hara, J. A., James, P. E., Panz, T., Grinberg, O. Y., Jain, N., Dunn, J., and Swartz, H. M. (1997b) Determining the anatomic position and histological effects in tumors of gloxy, an oxygen sensitive paramagnetic material, *Adv. Exp. Med. Biol.* **428,** 107-113.

Pace, R. J., and Chan, S. I. (1982) Molecular motions in lipid bilayers. III. Lateral and transversal diffusion in bilayers, *J. Chem. Phys.* **76,** 4241-4247.

Pajak, S., Cieszka, K., Gurbiel, R., Subczynski, W. K., and Lukiewicz, S. J. (1978) EPR measurements of the oxygen consumption by tumor cells, *Third meeting of the Polish Biophysical Society,* Wroclaw-Olesnica, Book of Abstracts, p. 70.

Pajak, S., Subczynski, W. K., Panz, T., and Lukiewicz, S. J. (1980) Rate of oxygen consumption of hamster melanoma cells as a factor influencing their radioresistance, *Folia Histochem. Cytochem.* **18,** 33-39.

Pasenkiewicz-Gierula, M., and Subczynski, W. K. (1996) Structure and dynamics of lipid bilayer membranes - comparison of EPR and molecular dynamics simulation results, *Curr. Top. Biophys.* **20,** 93-98.

Plachy, W. Z., and Windrem, D. A. (1977) A gas-permeable EPR sample tube, *J. Magn. Reson.* **21,** 237-239.

Pogue, B. W., O'Hara, J. A., Liu, K. J., Hasan, T., and Swartz, H. M. (1999) Photodynamic treatment of the RIF-1 tumor with verteporfin with online monitoring of tissue oxygen using electronic paramagnetic resonance oximetry, *SPEI* **3691,** 108-114.

Popp, C. A., and Hyde, J. S. (1981) Effects of oxygen on EPR spectra of nitroxide spin-label probes of model membranes, *J. Magn. Reson.* **43,** 249-258.

Povich, M. J. (1975 a) Measurements of dissolved oxygen concentrations and diffusion coefficients by electron spin resonance, *Anal. Chem.* **47,** 346-347.

Povich, M. J. (1975b) Electron spin resonance oxygen broadening, *J. Phys. Chem.* **79,** 1106-1109.

Reszka, K., and Sealy, R. C. (1984) Photooxidation of 3,4-dihydroxyphenylalanine by hematoporphyrin in aqueous solution: An electron spin resonance study using 2,2,6,6-tetramethyl-4-piperidone 1-oxyl (Tempone), *Photochem. Photobiol.* **39,** 293-299.

Rohmer, M., Bouvier, P, and Ourisson, G. (1979) Molecular evolution of biomembranes: structural equivalents and phytogenic precursor of sterols, *Proc. Natl. Acad. Sci. USA* **76,** 847-851.

Ryba, N. J. P., Horváth, L. I., Watts, A., and Marsh, D. (1987) Molecular exchange at the lipid-rhodopsin interface: spin-label electron spin resonance studies of rhodopsin-dimyristoylphosphatidylcholine recombinants, *Biochemistry* **26,** 3234-3240.

Sarna, T., and Sealy, R. C. (1984) Photoinduced oxygen consumption in melanin systems. Action spectra and quantum yields for eumelanin and synthetic melanin, *Photochem. Photobiol.* **39,** 69-74.

Sarna, T., Duleba, A., Korytowski, W., and Swartz, H. M. (1980) Interaction of melanin with oxygen, *Arch. Biochem. Biophys.* **200,** 140-148.

Singh, R. J., Hogg, N., Mchaourab, H. S., and Kalyanaraman, B. (1994) Physical and chemical interactions between nitric oxide and nitroxides, *Biochim. Biophys Acta* **1201,** 473-441.

Smirnov, A. I., Clarkson, R. B., and Belford, R. L. (1996) EPR linewidth (T_2) method to measure oxygen permeability of phospholipid bilayers and its use to study the effect of low ethanol concentrations, *J. Magn. Reson. B* **111**:149-157.

Smirnov, A. I., Norby, S. W., Clarkson, R. B., Walczak, T., and Swartz, H. M. (1993) Simultaneous multi-site EPR spectroscopy *in vivo, Magn. Reson. Med.* **30,** 213-220.

Smotkin, E. S., Moy, F. T., and Plachy, W. Z. (1991) Dioxygen solubility in aqueous phosphatidylcholin dispersion, *Biochim. Biophys. Acta* **1061,** 33-38.

Sotgiu, A. (1985) Resonator design for *in vivo* ESR spectroscopy, *J. Magn. Reson.* **65,** 206-214.

Stamler, J. S. (1995) in *Biochemical Pharmacological and Clinical Aspects of Nitric Oxide,* B. A. Weissman, N. Allon and S. Shapira, Eds., Plenum, New York, 67-78.

St. Denis, C. E., and Fell, C. J. (1971) Diffusivity of oxygen in water, *Can. J. Chem. Eng.* **49,** 885.

Stouch, T. R., and Bassolino, D. (1996) Movement of small molecules in lipid bilayers: Molecular dynamics simulation studies, in *Biological membranes,* K. Merz Jr. and B. Roux, Eds., Birkhauser, Boston, 255-280.

Strzalka, K., Sarna, T., and Hyde, J. S. (1986) ESR oximetry measurement of photosynthetic oxygen evolution by spin-probe technique, *Photobiochem. Photobiophys.* **12,** 67-71.

Strzalka, K., Walczak, T., Sarna, T., and Swartz, H. M. (1990) Measurement of time-resolved oxygen concentration changes in photosynthetic systems by nitroxide based ESR oximetry, *Arch. Biochem. Biophys.* **281,** 312-318.

Subczynski, W. K., and Hyde, J. S. (1981) The diffusion-concentration product of oxygen in lipid bilayers using the spin-label T_1 method, *Biochim. Biophys. Acta* **643,** 283-291.

Subczynski, W. K., and Hyde, J. S. (1983) Concentration of oxygen in lipid bilayer using a spin-label method, *Biophys. J.* **41,** 283-286.

Subczynski, W. K., and Hyde, J. S. (1984) Diffusion of oxygen in water and hydrocarbons using an electron spin resonance spin label technique, *Biophys. J.* **45,** 743-748.

Subczynski, W. K., and Hyde, J. S. (1998a) Membranes: barriers or pathways for oxygen transport, in *Oxygen Transport to Tissue XX, Advances in Experimental Medicine and Biology,* A. G. Hudetz, Ed., Plenum, New York, 399-408.

Subczynski, W. K., and Hyde, J. S. (1998b) Spin-label NO-metry in lipid bilayer membranes, in *Nitric Oxide in Transplant Rejection and Anti-Tumor Defense,* S. J. Lukiewicz and J. L. Zweier, Eds., Kluwer, Boston,, 95-107.

Subczynski, W. K., and Kusumi, A. (1985) Detection of oxygen consumption during very early stages of lipid peroxidation by ESR nitroxide spin probe method, *Biochim. Biophys. Acta* **821,** 259-263.

Subczynski, W. K., and Markowska, E. (1992) Effect of carotenoids on oxygen transport within and across model membranes, *Curr. Top. Biophys.* **16,** 62-68.

Subczynski, W. K., Hopwood, L. E., and Hyde, J. S. (1992a) Is the mammalian cell plasma membrane a barrier to oxygen transport?, *J. Gen. Physiol.* **100,** 69-87.

Subczynski, W. K., Hyde, J. S., and Kusumi, A. (1989) Oxygen permeability of phosphatidylcholine-cholesterol membranes, *Proc. Natl. Acad. Sci. USA* **86,** 4474-4478.

Subczynski, W. K., Hyde, J. S., and Kusumi, A. (1991a) Effect of alkyl chain unsaturation and cholesterol intercalation on oxygen transport in membranes: A pulse ESR spin labeling study, *Biochemistry* **30**, 8578-8590.

Subczynski, W. K. and Kusumi, A. (1985) Detection of oxygen consumption during very early stages of lipid peroxidation by ESR nitroxide spin probe method, *Biochim. Biophys. Acta* **821**, 259-263.

Subczynski, W. K. and Kusumi, A. (2003) Dynamics of raft molecules in the cell and artificial membranes: approaches by the pulse EPR spin labelling and single molecule optical microscopy, *Biochim. Biophys. Acta* **1610**, 231-243.

Subczynski, W. K., Lewis, R. N. A. H., McElhaney, R. N., Hodges, R. S., Hyde, J. S., and Kusumi, A. (1998) Molecular organization and dynamics of 1-palmitoyl-2-oleoylphosphatidylcholine bilayers containing a transmembrane helical peptide, *Biochemistry* **37**, 3156-3164.

Subczynski, W. K., Lomnicka, M., and Hyde, J. S. (1996) Permeability of nitric oxide through lipid bilayer membranes, *Free Rad. Res.* **24**, 343-349.

Subczynski, W. K., Lukiewicz, S., and Hyde, J. S. (1986) Murine *in-vivo* L-band ESR spin-label oximetry with a loop-gap resonator, *Magn. Reson. Med.* **3**, 747-754.

Subczynski, W. K., Markowska, E., and Sielewiesiuk, J. (1991b) Effect of polar carotenoids on the oxygen diffusion-concentration product in lipid bilayers. An ESR spin label study, *Biochim. Biophys. Acta* **1068**, 68-72.

Subczynski, W. K., Pasenkiewicz-Gierula, M., McElhaney, R. N., Hyde, J. S., and Kusumi, A. (2003) Molecular organization and dynamics of 1-palmitoyl-2-oleoylphosphatidylcholine membranes containing a transmembrane α-helical peptide with dynamic surface roughness, *Biochemistr.***42**, 3939-3948.

Subczynski, W. K., Renk, G. E., Crouch, R. K., Hyde, J. S., and Kusumi, A. (1992b) Oxygen diffusion-concentration product in rhodopsin as observed by a pulse ESR spin labeling method, *Biophys. J.* **63**, 573-577.

Subczynski, W. K., Wisniewska, A., Yin, J.-J., Hyde, J. S., and Kusumi, A. (1994) Hydrophobic barriers of lipid bilayer membranes formed by reduction of water penetration by alkyl chain unsaturation and cholesterol, *Biochemistry* **33**, 7670-7681.

Swartz, H. M. (2003) The measurement of oxygen *in vivo* using EPR techniques, in *Biological Magnetic Resonance* **18***: In Vivo EPR (ESR): Theory and Applications.* L.J. Berliner, Ed., Plenum Publishing Co., New York. 404-440.

Swartz, H. M., and Clarkson, R. B. (1998) The measurement of oxygen *in vivo* using EPR techniques, *Phys. Med. Biol.***43**, 1957-1975.

Swartz, H. M., and Glockner, J. F. (1989) Measurements of concentration of oxygen in biological systems in EPR techniques, in *Advance EPR in Biology and Biochemistry,* A. J. Hoff, Ed., Elsevier, Amsterdam, 753-782.

Swartz, H. M., and Glockner, J. F. (1991) Measurement of oxygen by ESRI and ESRS, in *Imaging and In Vivo EPR,* G. R. Eaton, S. S. Eaton and K. Ohno, Eds., CRC Press, Boca Roton, 261-290.

Swartz, H. M., Boyer, S., Gast, P., Glockner, J. F., Hu, H., Liu, K. J., Moussavi, M., Norby, S. W., Vahidi, N., Walczak, T., Wu, M., and Clarkson, R. B. (1991) *Magn. Reson. Med.* **20**, 333-339.

Swartz, H. M., Chen, K., Pals, M., Sentjurc, M., and Morse II, P. D. (1986) Hypoxia sensitive NMR contrast agents, *Magn. Reson. Med.* **3**, 169-174.

Swartz, H. M., Liu, K. J., Goda, F., and Walczak, T. (1994) India ink: a potential clinically applicable EPR oximetry probe, *Magn. Reson. Med.* **30**, 229-232.

Swartz, H. M., and Walczak, T. (1996) An overview of considerations and approaches for developing *in vivo* EPR for clinical applications, *Chem. Intermed.* **22**, 511-23.

Swartz, H. M., and Walczak, T. (1998) Developing *in vivo* EPR oximetry for clinical use, *Adv. Exp. Med. Biol.* **454,** 243-252.

Taie, S., Leichtweis, S., Liu, K. J., Miyake, M., Grinberg, O. Y., Demidenko, E., and Swartz, H. M. (1999) The effects of ketamine/xylazine and pentobarbital anesthesia on cerebral tissue oxygen tension, blood pressure, and arterial blood gas in rats, *Adv. Exp. Med. Biol.* **471,** 189-198.

Träuble, H. (1971) The movement of molecules across lipid membranes: A molecular theory, *J. Membr. Biol.* **4:**193-208.

Vahidi, N., Clarkson, R. B., Liu, K. J., Norby, S. W., Wu, M., and Swartz, H. M., 1994, *In Vivo* and *In Vitro* EPR oximetry with fusinite: A new coal-derived, particulate EPR probe, *Magn. Reson. Med.* **31,** 139-146.

Varghese, J. N., Laver, W. G., and Colman, P. M. (1983) Structure of the influenza glycoprotein antigen neuraminidase at 2.9 Å resolution, *Nature* **303**, 35-40.

Vaughn, M. W., Huang, K. T., Kuo, L., and Liao, J. C. (2001) Erythrocyte consumption of nitric oxide: Competition experiment and model analysis, *Nitric Oxide: Biology and Chemistry* **5**, 18-31.

Webster, R. G., Laver, W. G., Air, G. M., and Schild, G. C. (1982) Molecular mechanisms of variation in influenza viruses, *Nature* **296,** 115-121.

Wilson, I. A., Skehel, J. J., and Wiley, D. C. (1981) Structure of the hemagglutinin membrane glycoprotein of influenza virus at 3 Å resolution, *Nature* **289**, 366-378.

Windrem, D. A., and Plachy, W. Z. (1980) The diffusion-solubility of oxygen in lipid bilayers, *Biochim. Biophys. Acta,* **600,** 655-665.

Wisniewska, A., and Subczynski, W. K. (1998) Effects of polar carotenoids on the shape of the hydrophobic barrier of phospholipid bilayers, *Biochim. Biophys. Acta* **1368,** 235-246.

Wood, R. K., Dobrucki, J. W., Glockner, J. F., Morse II, P. D., and Swartz, H. M. (1989) Spectral-spatial ESR imaging as a method of noninvasive biological oximetry, *J. Magn. Reson.* **85,** 50-59.

Yin, J.-J., Pasenkiewicz-Gierula, M., and Hyde, J. S. (1987) Lateral diffusion of lipids in membranes by pulse saturation recovery electron spin resonance, *Proc. Natl. Acad. Sci. USA* **84**, 964-968.

Yin, J.-J., and Hyde, J. S. (1987) Spin-label saturation-recovery electron spin resonance measurements of oxygen transport in membranes, *Z. Phys. Chem. (Munich)* **153,** 57-65.

Zweier, J. L., Thompson-Gorman, S., and Kuppusamy, P. (1991) Measurement of oxygen concentration in the intact beating heart using electron paramagnetic resonance spectroscopy: a technique for measuring oxygen concentration in situ, *J. Bioenerg. Biomembr.* **23,** 855-871.